ACS APPLIED MATERIALS & INTERFACES

Forum Article

www.acsami.org

Polymer/Carbon Nanotube Nano Composite Fibers—A Review

Yaodong Liu and Satish Kumar*

School of Materials Science and Engineering, Georgia Institute of Technology, 801 Ferst Drive NW, MRDC-1, Atlanta, Georgia 30332-0295, United States

ABSTRACT: Carbon nanotubes (CNTs) are regarded as ideal filler materials for polymeric fiber reinforcement due to their exceptional mechanical properties and 1D cylindrical geometry (nanometer-size diameter and very high aspect ratio). The reported processing conditions and property improvements of CNT reinforced polymeric fiber are summarized in this review. Because of CNT polymer interaction, polymer chains in CNTs' vicinity (interphase) have been observed to have more compact packing, higher orientation, and better mechanical properties than bulk polymer. Evidences of the existence of interphase polymers in composite fibers, characterizations of their structures, and fiber properties are summarized and discussed. Implications of interphase phenomena on a broader field of fiber and polymer processing to make much stronger materials are now in the early stages of exploration. Beside improvements in tensile properties, the presence of CNTs in polymeric fibers strongly affects other properties, such as thermal stability, thermal transition temperature, fiber thermal shrinkage, chemical resistance, electrical conductivity, and thermal conductivity. This paper will be helpful to better understand the current status of polymer/CNT fibers, especially high-performance fibers, and to find the most suitable processing techniques and conditions.

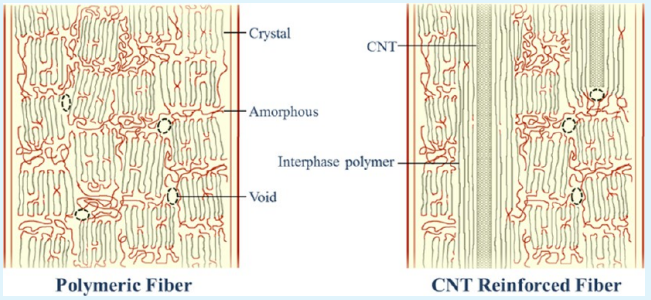

KEYWORDS: *carbon nanotube, composite, polymeric fiber*

1. INTRODUCTION

Natural fibers (silk, cotton) have been used in human life for thousands of years. However, the first man-made fiber (rayon) was manufactured only towards the end of 19th century. Later on, nylon was introduced to the world in 1939, and has gained great success in broad applications. Since then, more and more synthetic fibers have been developed and successfully commercialized, such as polyester fiber, acrylic fiber, and polyolefin fibers. Classified by their performance, synthetic fibers can be divided into conventional textile fibers and high-performance fiber with high modulus and tenacity that are engineered for specific uses.[1] The mechanical performance of fibers is the key factor for their structural applications and has been dramatically improved over the last century. Tensile strength of the commercial carbon fibers exceeds 5 GPa, which is about an order of magnitude higher than that of the strongest fiber made in a century ago. A further tensile strength improvement by another factor of ten is well within the realm of theoretical possibility. The higher tensile strength and modulus of a polymeric fiber are usually achieved by synthesizing new polymers, by improving the fiber's physical structures using better spinning method and drawing conditions, or by reinforcing the fiber using fillers with remarkable properties. Since the concept of nanotechnology emerged in the second half of the 20th century, many nanomaterials with exceptional or unique properties have been discovered or created. Of these nanomaterials, carbon nanotubes (CNTs) have gained intensive attention and interest to be used as reinforcement materials because of their extraordinary mechanical propertie and electrical and thermal conductivities.[2] Also, the high aspect ratio of CNTs that leads to anisotropic geometry makes them especially suitable to reinforce fibers. CNTs can be used to make pure CNT fiber or to reinforce polymeric, ceramic, and metallic fibers. Wholly CNT fibers have been processed from aqueous dispersions[3] and dispersions in strong acids,[4] drawn from CNT forests,[5] or pulled from CNT CVD reactor in the form of an aerogel fiber.[6] The highest tensile strength in a continuous CNT fiber of about 10 GPa has been measured at a gauge length of 1 mm.[7] Although this value sets a record for the strength of a continuous fiber, it is only a small fraction of the theoretical value.[8] Incorporation of CNTs into polymeric materials has been widely investigated over the last two decades. Many CNT containing polymer composites exhibiting significantly improved properties than neat polymers have been reported.[9−14] In this review, we summarize the studies on CNT-reinforced polymeric fibers including the dispersion methods of CNTs, improvements of fiber properties and structural changes after incorporating CNTs in polymeric fibers. It is also noted that infiltration of polymers into neat CNT fibers can enhances intertube stress transfer, and hence improves fiber tensile

Special Issue: Applications of Hierarchical Polymer Materials from Nano to Macro

Received: November 14, 2013
Accepted: January 27, 2014
Published: February 12, 2014

 © 2014 American Chemical Society dx.doi.org/10.1021/am405136s | *ACS Appl. Mater. Interfaces* 2014, 6, 6069−6087

Table 1. Summary of Various Literature Studies of Polymer/CNT Fibers

			key experimental factors									
					property improved by the addition of CNTs[e]					characterization[e]			
polymer[a]	spinning method[b]	CNT dispersion method[c]	CNT type[d]	wt_{Max} (wt %)	tensile property	thermal stability	electrical conduct	thermal conduct	chemical resistance	fiber structure	thermal transition	thermal shrinkage	ref
PAN	DJ-wet	sonication, evaporation	S	10	↑						↑	↓	56
			M	20						●	↑	↓	53
	gel		S,M	5	↑	↑					↑	↓	52
			F	1	↑				↑	●	↑		49
			F	1	↑					●			122
	elec	co-solvent	S	4	↑					●			123
			S,M	1						●			124
		sonication	M	16				↑					81
		co-solvent	f_1-M	35	↑					●		↓	60
			f_1-M	0.5			↑			●			125
PE	melt	ball milling →melt mixing +sonication	f_2-M	0.5									126
		melt mixing	M	5	↑					●	↑		38
	elec		M	1	↑								127
		co-solvent +sonication	S	6	↑					●			128
	gel		M	2.5	↑						↑		129
			M	2.5	↑					●			58,130
		poly-sol+sonication	S	2	↑					●			131
		poly-sol+sonication	f_o-M	3	↑	↑							132
			f_1-M	5	↑						↑		133,134
PVA	elec	poly-sol	f_1-M	7.5	↑								135
				3	↑					●			136
		poly-sol +polyelectrolytes +sonication	M	5	↑								137
		poly-sol+sonication	S	10	↑						↑		138
	wet		M	4.5	↑	↑				●	↑		89
			M	40			↑						68
	gel	surfactant+sonication	S, M	1	↑		↑						139
		co-solvent +sonication +homogenizer (with temperature and shear flow control)	S	10	↑					●			109
		co-solvent+homogenizer	S	0.3	↑					●			108
		co-solvent+sonication	f_o-M	1	↑					●			140
			S	3	↑					●	↑		106
			S	1	↑					●	↑	↓	42
	coag	surfactant+sonication	M	11			↑						141
			S	15	↑								142
			S	21	↑								143,144
			M	60	↑		↑						145
PA	melt	dry mixing (blender)	M, f_o-M	1	↑						↑		146
		melt mixing	M, f_o-M	2	↑		↑						147
			M	7	↑								148
			M	10	↑	↑				●	↑		31

dx.doi.org/10.1021/am405136s | ACS Appl. Mater. Interfaces 2014, 6, 6069−6087

Table 1. continued

polymer[a]	spinning method[b]	CNT dispersion method[c]	key experimental factors: CNT type[d]	wt_{Max} (wt %)	property improved by the addition of CNTs[e]: tensile property	thermal stability	electrical conduct	thermal conduct	chemical resistance	characterization[e]: fiber structure	thermal transition	thermal shrinkage	ref
			f_o-M	2	↑	↑				●	↑		149
		in situ	f_1-S	1.5	↑	↑				●			150
	elec	poly-sol+sonication	f_o-M	2.5	↑	↑				●	↑		151
			f_o-M	7.5	↑	↑				●	↑		57
PU	melt	in situ	f_1-M	7						●	↑		152
			f_1-M	5						●			153
		melt mixing	M	3			↑						66
PMMA	melt	dry mixing→melt mixing	C	10	↑	↑					↑	↓	54
	elec	sonication	f_o-M	5	↑					●			154
PMMA/CNT (S−C)	c-elec	surfactant+sonication	M				↑			●			85
Pitch	melt	melt mixing	f_1-M	0.3	↑					●	↑		155
		sonication, evaporation	S	10	↑		↑						156
PET	melt	sonication→mixing with melt→evaporation	S	2	↑								157
		melt mixing	S	1	↑	↑					↑		33
			M	7						●			55
		dry mixing→melt mixing	C	5	↑	↑				●	↑		158
PBO	DJ-wet	in situ	S	10	↑	↑						↓	115
			f_1-M	8	↑	↑				●			159
			f_1-M	1.5	↑	↑							160
			f_o-M	0.54	↑	↑	↑			●			161
PAni	wet	poly-sol+sonication	S	2	↑		↑						61
			S	0.76	↑								162
cellulous	DJ-wet	ionic liquid-grinding	M	9	↑	↑				●			90
			M	10	↑		↑			●		↓	59
Cel/CNT (S−C)	DJ-c-elec	ionic liquid-grinding	M	45	↑	↑	↑			●			84
PP	melt	melt mixing	C	5	↑								163
			M	1	↑	↑				●	↑		88
		compabilizer/evaporation[f]→melt mixing	f_1-S/M	1	↑					●	↑		26
		co-solvent+sonication→melt mixing	S, f_o-S	10	↑								164,165
		surfactant+polymer powder[g]→melt mixing	M	5	↑					●			166
		evaporation	S	1	↑								167
			S	2	↑								168
PVDF	elec	sonication	M	2.8						●			169
	melt	melt mixing	f_3-F	0.01						●			170
lignin	elec	co-solvent+sonication	M	6	↑		↑			●			171
PEK	DJ-wet	in situ	F	20	↑		↑			●	↑	↓	69
			F	28				↑					82
PEI	coag	aqueous+surfactant+sonication	S	75	↑		↑				↑		172

dx.doi.org/10.1021/am405136s | ACS Appl. Mater. Interfaces 2014, 6, 6069−6087

Table 1. continued

			key experimental factors									
					property improved by the addition of CNTs[e]					characterization[e]			
polymer[a]	spinning method[b]	CNT dispersion method[c]	CNT type[d]	wt_{Max} (wt %)	tensile property	thermal stability	electrical conduct	thermal conduct	chemical resistance	fiber structure	thermal transition	thermal shrinkage	ref
PI	melt	melt mixing	S	1	↑								173
	melt	melt mixing	M	0.5	↑					●			174
PC	melt	melt mixing	M	2	↑								72
PBT	elect.	sonication	M	4	↑						↑	↓	175
PVAc	elec	poly-sol+sonication	M, f_1-M	5			↑						176
PEO	elec	surfactant+sonication	M	6						●			177
PVP	elec.	poly-sol+sonication	M	4			↑				↑		178
PAni+ PEO	elec	co-solvent	f_o-M	100			↑						179
			f_1-M	5	↑		↑			●			180
PAni+PP	melt	melt mixing	M	7.5		↑	↑				↑		64
PE+PP	melt	melt mixing	M	4.2	↑		↑						63
PP+PA	melt	melt mixing	M	5	↑	↑	↑				↑		181
Vectra	melt	solution-premixing, then melt mixing	f_1-M	1	↑	↑				●	↑		114

[a]Polymer abbreviations: PAN, polyacrylonitrile; PE, polyethylene; PVA, poly(vinyl alcohol); PA, polyamide; PU, polyurethane; PMMA, poly(methyl methacrylate); PET, polyethylene terephthalate; PBO, poly(*p*-phenylene benzobisoxazole); PAni, polyaniline; PP, polypropylene; PEK, poly(ether ketone); PEI, polyethyleneimine; PI, polyimide; PC, polycarbonate; PVAc, poly(vinyl acetate); PEO, polyethylene oxide; PEI-C, poly(ethylenimine) catechol; PBT, poly(butylene tere-phthalate); PVDF, polyvinylidene fluoride; PVP, polyvinylpyrrolidone; Vectra, random aramid copolymer of *p*-hydroxyben-zoic acid and 2-hydroxy-6-naphthoic acid; (S−C), sheath and core structure. [b]Spinning method abbreviations: melt, melt-spinning; Elec, electro-spinning; c-Elec, coaxial electro-spinning; D-Elec, dry-jet wet electro-spinning; Gel, gel-spinning; Coag, coagulation spinning; wet, wet-spinning; DJ-Wet, dry-jet wet-spinning. [c]CNT dispersion method abbreviations: evaporation, CNT is dispersed in a solvent good for both CNT and polymer at low concentration by ultra-sonication, then CNT dispersion is added into polymer solution, and the excess solvent is removed by evaporation under vacuum or not, the above procedure is repeated until reach desired CNT concentration; co-solvent, CNT is dispersed in a solvent good for both CNT and polymer, including DMF and DMSO; solvent, CNT is dispersed in a good solvent good for CNT; poly-sol, CNT is dispersed in a solvent good for polymer but poor for CNT; sonication, CNT is dispersed in a solvent using ultra-sonication; melt mixing, CNT is mixed with polymer melt by mechanical methods, such as twin-screw and melt-mixer; surfactant, surfactant is used to disperse CNT in a solvent good for polymer with ultra-sonication; in situ, in situ polymerization of polymer with CNTs, CNT is added to monomer solution followed with polymerization to form composite solution. [d]CNT type: S, SWNT; F, few wall NT; M, MWNT; C, carbon nanofiber; f, functionalized (f_1, oxidized in strong acid solution, f_2, UV Ozone treatment, f_3, amine functionalized, f_o, other methods). [e]Symbols: ↑ increase; ↓ decrease. [f]A compabilizer polymer, here PP-g-MA, is dissolved in xylene, and functionalized CNT is dispersed in butanol; CNT is added into PP-g-MA using evaporation method, and then composite solution is vacuum dried. [g]CNT is dispersed in a solvent by ultrasonication, then mixed with polymer powder, and finally vacuum dried to composite powders.

dx.doi.org/10.1021/am405136s | ACS Appl. Mater. Interfaces 2014, 6, 6069−6087

properties. The studies of polymer-infiltrated CNT fibers are beyond the scope of this review, as these fibers tend to be compared with carbon fibers instead of polymeric fibers.

2. COMPOSITE FIBER PROCESSING

Polymer/CNT fibers have been spun using melt and solution spinning as well as electrospinning techniques. One of the crucial processing issues is how to achieve homogeneous dispersion of debundled CNTs in polymer matrices.[15] CNTs, particularly small-diameter CNTs, have the propensity to aggregate into bundles or ropes because of their ubiquitous intertube van der Waals forces. The shear modulus of individual SWNT is as low as ~1 GPa, which is far below its axial tensile modulus.[16] Axial tensile modulus depends on the tube diameter, and can vary between about 400 GPa to about 1 TPa.[17] The relatively low shear modulus can make the SWNT rope relatively flexible,[16] despite its high tensile modulus. Additionally, the formation of CNT bundles leads to significant reduction of CNT surface area.[18] For CNT-reinforced composite, if CNTs are dispersed in bundles instead of exfoliated individual tube, the interfacial area between CNT and polymer matrix will be dramatically reduced. For example, the surface area of 9 nm bundles of SWNTs (outer diameter 1 nm) is only 21.3% of the surface area of individual SWNT of the same diameter and same mass. The interfacial area between CNT and polymer was observed to play a fundamental role in the reinforcement mechanism.[19] Therefore in those cases where property improvements depend on the surface interaction between CNT and the polymer, 5 times more quantity of SWNTs will be required for a composite if they were dispersed as 9 nm diameter bundles rather than as 1 nm diameter individual tube in the polymer. The good dispersion of CNTs in a polymer matrix can be important to fully utilize their exceptional properties. Therefore, the processing method of dispersing CNTs is one of the most important steps to obtain high quality composites.

Spinning methods, CNT dispersion conditions and characterizations of various polymer/CNT composite fibers from literatures are summarized in Table 1. How to disperse CNTs in small bundle size or individual tube is a big challenge for composite fiber processing. Although it has also been reported that CNTs can be spontaneously dissolved in some solvents using surface protonation[4,20,21] and surface reduction,[22] or can be dispersed in ionic liquids by slight agitation,[23] these solvents are not always suitable for CNT dispersion in polymers. To improve the dispersion of CNTs in polymer matrices, surfactant, covalent functionalization, as well as noncovalent functionalization have been employed. However, if the surfactant and functionalizing groups remain in the ultimate fiber, they will be at the CNT polymer interface and could potentially have a negative effect on the composite system. In the case that direct CNT polymer interaction is preferred, the usage of surfactants or functionalization should be carefully considered. Additionally, covalent functionalization and grafting will create defects on the CNT surface, which lowers both electrical and thermal conductivity as well as mechanical properties of CNTs. Even though functionalization has above mentioned shortages, about 30 % of reported composite fiber studies (Table 1) used various functionalization methods to modify CNT surface. These methods include acid oxidation, ozone treatment, amine functionalization, and polymer grafting. The functionalization of CNT surface may be helpful in achieving better CNT dispersion in polymer matrices that will lead to increased CNT polymer interfacial area. If CNTs cannot be debundled or dissolved spontaneously, techniques such as mechanical agitation, shear, and sonication are used to achieve their dispersion in the polymer melt or solution. For examples, ball milling was performed to mix polymer powder with CNT particles, extruder or melt-mixer was adopted to distribute CNTs in polymer melt, mechanical stirring, microfluidization, sonication, and homogenization were used to disperse CNTs in a solvent or polymer solution (source from Table 1). It is known that the CNT length will be shortened during intensive mechanical shear. A study of length and diameter changes of SWNT bundles processed by microfluidization or horn sonication clearly showed that CNT length was significantly shortened even though CNT bundle diameter was reduced after prolonged processing durations (Figure 1).[24] The long

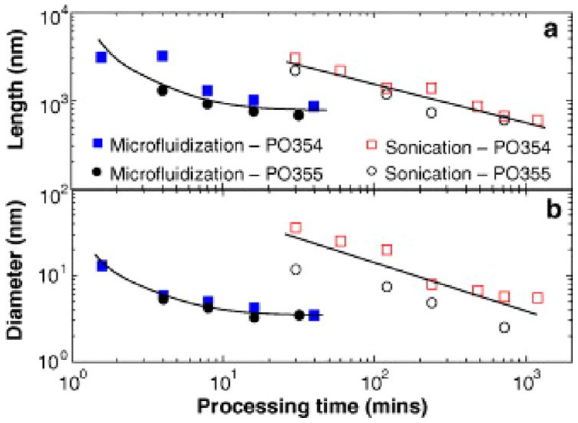

Figure 1. Effects of horn sonication and microfluidization on SWNT length and bundle diameter. (a) bulk average length, (b) bulk average diameter. PO354 and PO355 are different types of HiPCO tubes. Solid lines are for guidance only. Reprinted with permission from ref 24. Copyright 2010 Elsevier.

CNT length in composites is important for the stress transfer between polymer matrix and CNT.[10,25] Although extensive efforts have been devoted on the dispersion methods of CNTs, how to exfoliate CNTs while preserving CNT length is still a significant issue and challenge for fabricating a composite which can effectively utilize the exceptional properties of CNTs. Also, it should be noted that the radius of curvature and chirality of CNT surface layers could affect their interactions with the surrounding polymer and thus may affect the composite properties. However, to the best of our knowledge, no study has been reported regarding these factors.

3. ADVANTAGES OF CNTS IN POLYMERIC FIBERS

The addition of CNTs in polymeric fibers has been shown to affect their physical structures, enhance tensile properties, reduce fiber thermal shrinkage, improve chemical resistance, increase electrical and thermal conductivities, and lead to higher polymer thermal transition temperature. Processing and properties of various polymer/CNT fibers are summarized in Table 1, and details of some of these studies are also discussed in the following sections.

3.1. Polymer Crystallization, Interphase Formation, and Tensile Properties. CNTs have been reported to act as the nucleating agent for polymer crystallization as well as the template for polymer chain orientation. The long length, nanometer size diameter, substantial surface area, and high

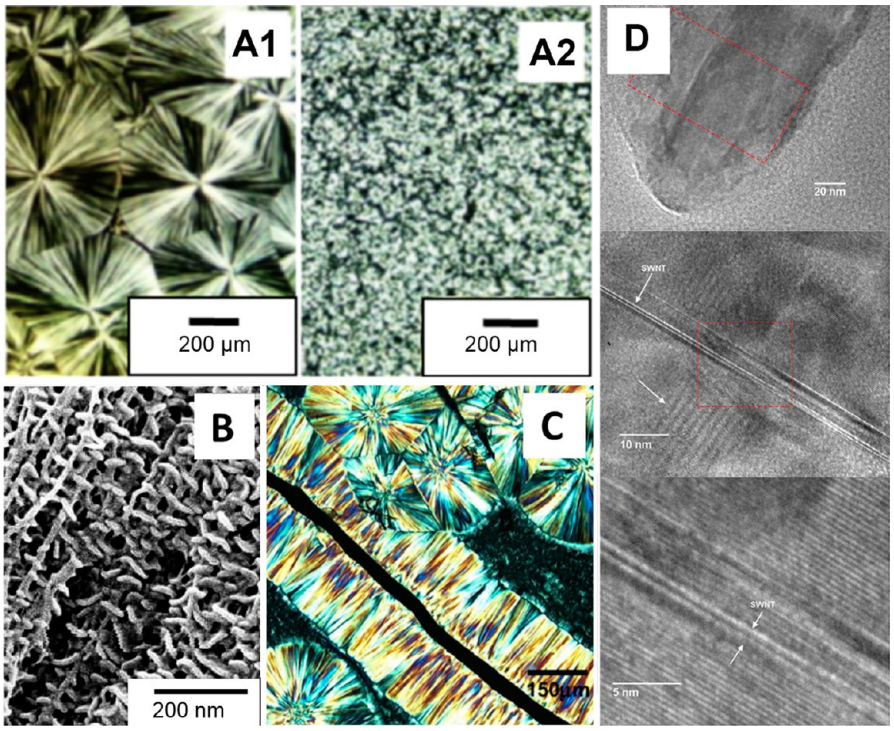

Figure 2. Cross-polarized optical micrographs of (A1) PP and (A2) SWNT/PP with 1 wt % SWNT bulk samples melted at 220 °C and cooled to room temperature at a rate of 0.5 °C/min. Reprinted with permission from ref 26. Copyright 2008 Elsevier. (B) UHMWPE forms aligned shish-kebab structure on MWNTs after controlled solution crystallization. Reprinted with permission from ref 37. Copyright 2013 American Chemical Society. (C) Polarized optical micrograph of transcrystalline interphase layer of PP surrounding the CNT fiber. Reprinted with permission from ref 39. Copyright 2008 Elsevier. (D) Transmission electron micrographs of self-assembled PVA/SWNT nano fibril. Nano fibril diameter is about 120 nm. SWNT and PVA (200) lattice planes (*d*-spacing ~0.385 nm) parallel to SWNT axis can be observed. Reprinted with permission from ref 40. Copyright 2006 Elsevier.

aspect ratio make CNTs, especially SWNTs, distinct from other known nucleating agents. Figure 2A shows the cross polarized optical images of crystallized polypropylene (PP) and PP/SWNT (1 wt %) bulk samples. It was observed that the spherulite diameter of PP crystals decreased from 400 to 20 μm after adding 1 wt % CNT, which suggested the strong nucleation effect of CNT on PP crystallization.[26] The nucleating effect of CNT besides PP[27−29] has also been observed for many other polymers including poly(vinyl alcohol) (PVA),[30] polyamide,[31] polyethylene (PE),[32] and polyethylene terephthalate (PET).[33] Because of CNT's nucleation effect, polymer crystallization temperature is normally shifted to a higher temperature and crystallization rate becomes much faster in CNT containing polymers than in neat polymer. In melt spun PET fibers, the PET crystallization temperatures measured by DSC cooling method increased from 200 to 209 to 214 °C when CNT concentrations increased from 0 to 0.1 to 1 wt %,[34] respectively. Also for the melt blended PP/SWNT composite, the addition of 0.8 wt % SWNT increased the PP isothermal crystallization rate at 125 °C from 1.8×10^{-8} to 4.2×10^{-5} s^{-1}.[28] For solution-crystallized PP on dispersed MWNTs, the formed PP-coated CNT particles had a high degree of crystallinity of ~80 %, and this high level of crystallinity was ascribed to the nucleation effect of CNTs, which led to more complete PP crystallization.[35]

The nanometer size diameter, cylindrical shape, long aspect ratio, and graphitic surface of CNTs make it possible for the polymer chains to align along the CNT axis. It has been observed that PE and nylon-6,6 formed kebab-like structures along CNT axis by solution crystallization.[36] In these cases, CNT serves as shish and orient the growth direction of polymer lamellas perpendicular to CNT's axis. Such observations have been reported by a number of researchers. Figure 2B shows a highly oriented periodic kebab-like PE crystals on MWNTs in an aerogel MWNT fiber after solution crystallization.[37] For melt spun PE/MWNT fibers, when amorphous PE phase was removed by chemical etching, Fu et al. observed the formation of kebab structure with CNT as shish.[38] Additionally, an isothermally crystallized PP sample shows the formation of a trans-crystalline PP layer on the surface of CNTs (Figure 2C).[39] CNTs may also align polymer chains along their axes. For example, self-assembled PVA fibrils formed under shear in PVA solution were isotropic, whereas self-assembled PVA fibrils formed under similar conditions from solution containing small amount of CNTs exhibited high degree of PVA orientation.[40] Minus et al. observed that PVA chains are oriented parallel to the SWNT axis when PVA solution crystallizes in the presence of SWNTs (Figure 2D).[41] Additionally, in gel-spun PVA/CNT fiber, the average crystal size of PVA along chain axis (010) direction was 8.4−14.8 nm as measured by WAXD; whereas, the PVA crystal in the vicinity of CNTs was as large as more than 40 nm long along CNT axis as measured from high resolution TEM images.[42] From these studies, it is clear that CNTs may act as templates for polymer orientation. The interaction between CNT and polymers leads to microstructural development of polymers in the vicinity of CNTs different than that in polymer matrix, and this interphase polymer could possess much better properties than polymer in the bulk. To fully realize the positive effects of CNTs, the

Table 2. Polymers, CNT Types, CNT Contents, and the Calculated CNT Modulus Reinforcement Efficiency[a]

polymer/matrix	CNT type	CNT content (wt %)	Y_m (GPa)	Y_c (GPa)	dY_c/dV_f (GPa)[c]	ref
PVA	SWNT	10	21.8	119.1	>1540	2013[109]
PVA	SWNT	1	48	71	~2740	2009[42]
PAN- carbonized	SWNT	1[b]	302	450	~6500	2007[100]
PVA	DWNT	0.2	2	3.6	~1240	2004[10,19]
PMMA	SWNT	0.014	3.1	3.9	~9600[d]	2004[182]
PAN- carbonized	SWNT	4	66.2	138	~2560	2003[123]
SU-8 resin	MWNT	0.1	4.2	5.0	~1300	2002[183]
pitch- carbonized	SWNT	5	33	78	~1200	1999[156]

[a] Y_c is Young's modulus of the composite, Y_m is Young's modulus of matrix. dY_c/dV_f is calculated on the basis of the rule of mixture, V_f is volume fraction of CNT. [b] CNT content in PAN precursor fiber. The CNT content increases to ~2 wt % after carbonization. Density of SWNT and carbon fiber are assumed to be (1 nm diameter tube rope) 1.52 g/cm^3 and 1.8 g/cm^3, respectively. [c] For dY_c/dV_f calculations in this table, it was assumed that CNTs have ideal orientation along the fiber axis, and that the properties of the polymer matrix in the composite fiber are the same as that in the control fiber containing no nanotubes. [d] On the basis of elastic modulus at a frequency of 100 rad/s at 25 °C, the dY_c/dV_f increases to ~24 000 GPa when temperature decreases to −150 °C.

optimal processing conditions of polymer/CNT composite fibers can be different from the neat polymer processing conditions.

Previous studies on CNT reinforced polymeric fibers exhibit substantial improvements, such as tensile properties, thermal stability, electrical conductivity, thermal conductivity, chemical resistance, polymer thermal transition temperatures and polymer structural parameters (crystallinity, crystal size, and orientation) (Table 1). These reinforcements of polymeric fibers with the addition of CNTs can be divided into two sections: (1) intrinsic properties of CNTs, such as electrical conductivity, tensile properties and thermal conductivity; (2) templating effect of CNTs on polymers. If a composite fiber is considered as the simplest model consisting polymer matrix phase and aligned fiber phase, based on well-known rule of mixture (Voigt model),[43] the composite tensile modulus along fiber axis can be calculated by

$$Y_c = (Y_f - Y_m)V_f + Y_m \quad (1)$$

Where Y_c is the Young's modulus of the composite, Y_f is the Young's modulus of the filler, Y_m is the Young's modulus of the polymer matrix, and V_f is the volume fraction of the filler. The reinforcement of modulus derived from eq 1 is then

$$\frac{dY_c}{dV_f} = Y_f - Y_m \quad (2)$$

If $Y_f \gg Y_m$, the following approximation becomes valid.

$$Y_f - Y_m \approx Y_f \quad (3)$$

For CNT-reinforced composite fibers, the CNT reinforcement efficiency of modulus can be calculated by dY_c/dV_f. In most studies the values of dY_c/dV_f were in the range of 10 to 400 GPa, whereas in some studies, the values were in the range of 600−800 GPa.[10,20] In few cases, the tensile modulus reinforcement values of CNT were even higher than 1000 GPa (Table 2). Here we note that the axial tensile modulus of CNTs is in the range of about 500−1000 GPa, which depends on the nanotube diameter and the number of walls in the tube, whereas the specific tensile modulus (material's Young's modulus divided by its density) of CNTs is 469 N/tex and is independent of the tube diameter and number of walls.[17] The calculations in Table 2 based on eq 2 assume that the properties of the polymer matrix in the composite fiber are the same as that in the control fiber containing no nanotubes. It is noted that these calculations in Table 2 ignore the length distribution and orientation of CNT, which will lower CNT's reinforcement.[44−46] Because CNT used in composite consists of tubes with various lengths and orientation directions, the dY_c/dV_f calculated from eq 2 will be much lower than the theoretic modulus of CNT if the reinforcement only comes from the intrinsic properties of the added CNT. Polymer/CNT composites, in Table 2, have calculated values of dY_c/dV_f higher than the theoretic modulus of CNTs, which indicate that the reinforcement of tensile modulus is ascribed to not only the intrinsic properties of CNT but also the improvements of polymer physical structures. The polymers close to the surface of CNT have significantly better chance to be affected by CNT other than the polymer far away from CNTs. Thus, the results shown in Table 2 indicate the existence of interphase polymer with much better properties than the polymer matrix in these composites.

The nucleation and template effects induced by the interactions between CNT and polymer will affect the structure of the interphase polymer. There have been many studies showing that polymer in the vicinity of carbon nanotubes has more compact chain packing, better chain alignment and enhanced mechanical properties than the bulk polymer. Ding et al. observed the existence of polymer sheath (~50 nm thick) on MWNT surface that protruded on MWNT/polycarbonate (PC) composite fracture surface (Figure 3A, B).[47] Figure 3C shows that when this sheath layer contacted with AFM tip, the outer polymer layer suddenly contracted and balled up. The formation of polymer sheathing layer on MWNTs clearly showed the strong CNT−polymer interaction. Barber et al. measured the interfacial strength between CNT and polyethylene−butane (PEB) matrix through CNT pullout experiment by AFM measurement using a single MWNT as tip.[48] They found that the polymer in the vicinity of CNT was able to withstand an average interfacial stress of 47 MPa, whereas the bulk PEB is normally reported to yield at a stress of less than 10 MPa. In an early study on highly oriented PP/CNT films, Shaffer et al. examined PP crystals close to and away from carbon nanofibers (CNFs) by TEM and qualitatively concluded that crystals in CNT's vicinity had a shorter inter-lamellae spacing and a higher crystallinity than crystals farther away from CNT.[27] For CNT-reinforced PAN fibers, Chae et al. observed the existence of highly oriented PAN chains in the vicinity of SWNT using high-resolution TEM (Figure 4A).[49] Figure 4B shows Raman G-band spectra of PAN/SWNT fibers at laser polarization angles parallel and perpendicular to fiber axis. The

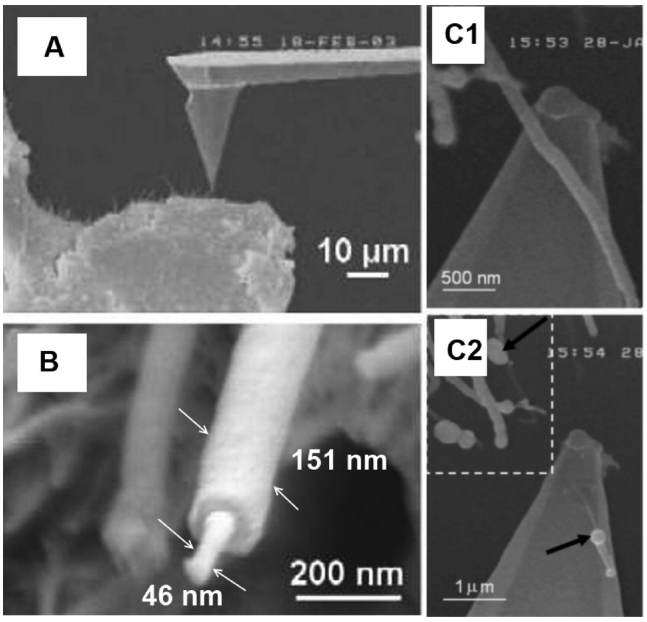

Figure 3. (A) Far-field SEM image of the nanomanipulation experiment inside the Hitachi S4500 SEM. (B) High-resolution images (LEO 1525) of nanotube structures coated with the polymer sheath protruding from the MWCNT−polycarbonate fracture surface. (C) SEM time-lapsed images of balling up of the polymer sheath (C1) before and (C2) after contact with the AFM tip. Reprinted with permission from ref 47. Copyright 2013 American Chemical Society.

Raman G-band peak intensity ratio was 42 based on Figure 4B suggesting high degree of SWNT alignment along the fiber axis after drawing. Additionally, the equatorial *d*-spacing in gel-spun PAN fiber decreased with the incorporation of SWNTs in comparison to neat PAN fibers (Figure 4C). These results suggest that CNT orients PAN crystal conformation in its vicinity and extends PAN chains along its axis.[49,50] In brief, it is obvious that the addition of CNTs strongly affect the microstructure polymer development in its vicinity. In addition to microstructural improvement of interphase polymer, improvements in macroscopic properties of composite fibers have also been observed with the addition of CNTs. It is known that the orientation and configuration of polymer chains are critical for the fiber performance.[51] The overall Herman's orientation factor of polymer crystals characterized by WAXD increased from 0.4 to 0.7 in PE fiber by adding 2 wt % SWNTs,[32] from 0.73 to 0.88 in PP fiber by adding 1 wt % SWNT[26] and from 0.52 to 0.62 in PAN fiber by adding 1 wt % FWNT.[52]

The formation of highly ordered interphase polymer is generally advantageous for the tensile properties of the composite fiber in two ways: (i) the presence of interphase polymer is expected to strengthen the stress transfer between CNT and the polymer. (ii) The highly ordered interphase polymer is expected to have higher mechanical properties than the bulk polymer, thus resulting in overall increase in properties. In Table 2, the tensile property improvements in composites are thought to come from both the CNT and the interphase polymer. Tensile property improvements in composite fibers can in principle be achieved by increasing CNT loading and by promoting the formation of interphase polymers. However, in the studies conducted to date, the CNT loadings in the composite fibers have been somewhat limited. High CNT loading typically causes CNT aggregation,[53−55] and therefore may be detrimental to the ultimate fiber properties. Controlling and improving the formation of interphase polymer remains an important pathway by which composite fiber properties can be improved. The volume fraction of interphase polymer depends on the CNT−polymer interfacial area, intertube distance, and the thickness of the interphase layer. Figure 5 shows the cross-section schematics of composite fibers with perfectly aligned CNT. The exfoliation of CNT from bundled to individual tubes dramatically increases CNT polymer interfacial area. The small interphase regions could overlap to form a larger interphase regions constituting of highly ordered polymer. Assuming that SWNTs of 1.2 nm are used to reinforce the polymeric fiber, and that the interphase layer thickness is 10 nm, then 0.435 vol % fully exfoliated and perfectly aligned SWNT in a fiber can effectively covert the entire polymer volume into an interphase region. It is noted that 10 nm is a typical crystal size in fibers such as gel-spun PAN[49] and PVA fiber,[42] and therefore interphase formation of such a size is not unexpected. If the interphase layer thickness can be increased to 20 nm, SWNT concentration of as low as 0.11 vol % in a polymeric fiber can turn the entire polymer matrix into the ordered interphase. With the formation of large volume fraction of interphase, a dramatic improvement in fiber tensile properties can be expected.

3.2. Effect on Thermal Transition Temperature. Figure 6A shows that the dynamic mechanical tan(δ) peak temperature of solution-spun PAN fibers shifted from 103 to 116 to 143 °C when SWNT weight fraction increased from 0 to 5 to 10 wt %, respectively. Additionally, the magnitude of tan(δ) peak decreased significantly and the peak became broader towards higher temperatures with increasing CNT loading.[56] The decrease of the tan(δ) peak intensity can be attributed to the increased interactions between CNTs and polymer chains. Comparing PAN and PAN/SWNT (10 wt %) fibers, the storage modulus especially at high temperature is significantly improved (Figure 6B). For gel-spun PAN fibers, the glass transition activation energy increased from 544 to 717 to 809 kJ/mol and β_c transition temperature measured at 10 Hz increased from 75 to 78 to 80.4 °C when CNT loading increased from 0 to 0.5 to 1 wt %, respectively.[49] Besides PAN fibers, the up-shift of tan(δ) peak temperature was also observed in number of other polymer/CNT fibers, such as nylon-6,6 (from 85 to 92 °C with the addition of 7.5 wt % MWNT),[57] PE (from 70 to 120 °C with the addition of 0.25 wt % MWNT),[58] PVA (from 100 to 114 °C with the addition of 10 wt % SWNT,[35] from 86 to 93 °C with the addition of 1 wt % SWNT[42]), and PP (from −5 to 7 °C with the addition of 1 wt % MWNT).[26]

3.3. Polymer Shrinkage and Orientation above Glass-Transition Temperature. When an oriented textile polymeric fiber is heated to a temperature above its glass-transition temperature (T_g), amorphous polymer chain segments will gain mobility and the fiber length will shrink due to entropic force. The incorporation of CNT in many polymeric fibers has been observed to restrict and reduce fiber's entropic shrinkage, such as, PP,[26] cellulose,[59] PVA,[42] and PAN fibers.[50,52,53,60] Figure 7A shows the shrinkage of PP and PP/SWNT fibers. The PP fiber shrinkage after being heated to 160 °C was greatly reduced from 28 to 5 to 2% when the addition of SWNT in fibers increased from 0 to 0.1 to 1 wt %, respectively.[26] Beside entropic shrinkage, the addition of CNTs in polymeric fibers can also reduce the shrinkage caused by chemical reactions. For homo-polymer PAN fibers heated in nitrogen, the reaction

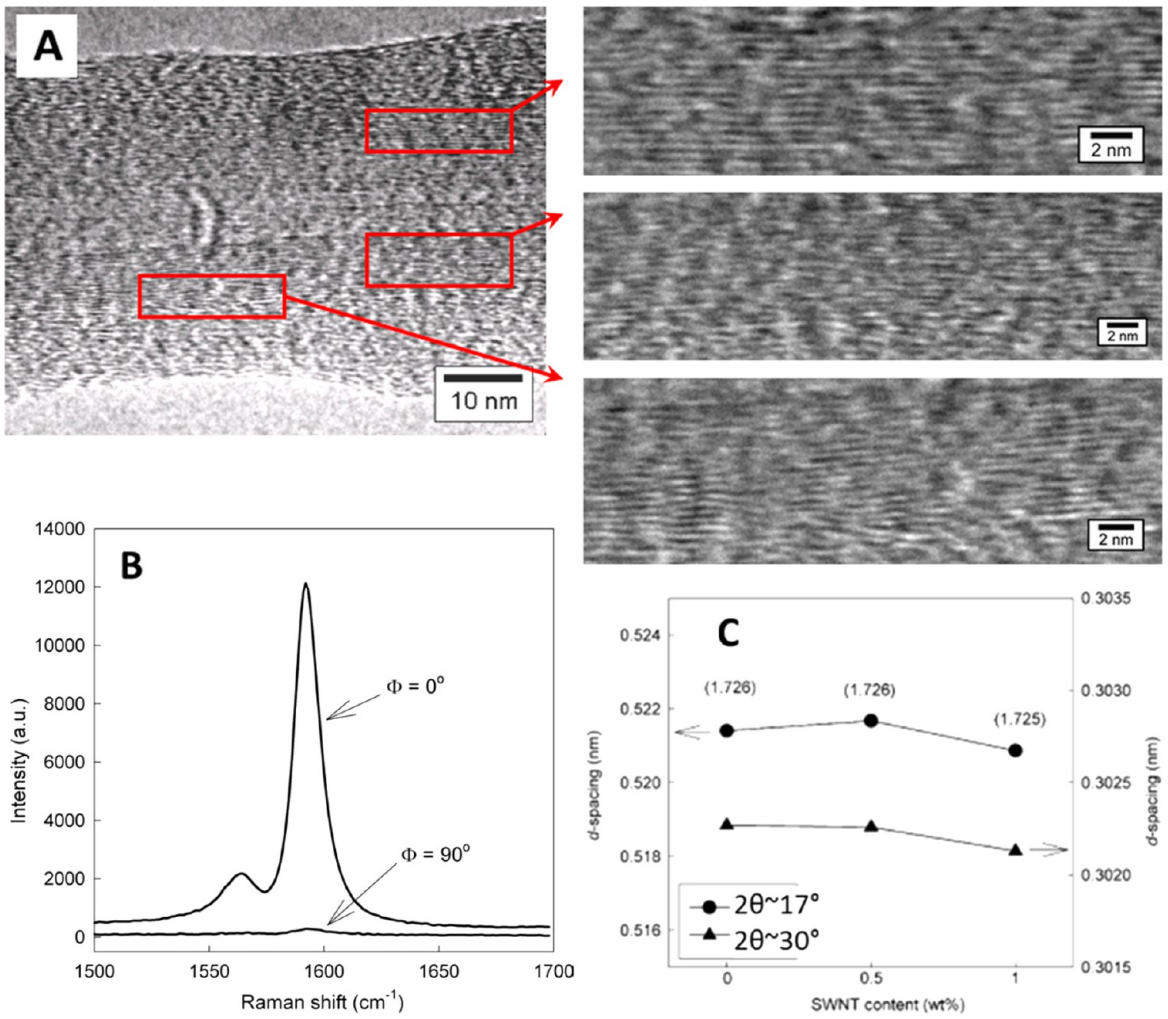

Figure 4. Structural studies in gel spun PAN/SWNT (99/1 wt/wt) fiber. (A) High-resolution TEM PAN lattice images in the vicinity of CNT in a fibril showing highly ordered PAN molecules. (B) G-band Raman spectra for PAN/SWNT (1 wt %) fiber. The angle between polarizer and the fiber axis are 0 and 90°. (C) Change in PAN equatorial *d*-spacings ($2\theta \approx 17$ and 30°) when 0.5 and 1 wt % SWNT are in the fiber. In both cases, the equatorial *d*-spacing of compposite fibers is reduced as compared to the PAN fiber without CNT. Reprinted with permission from ref 49. Copyright 2006 Elsevier.

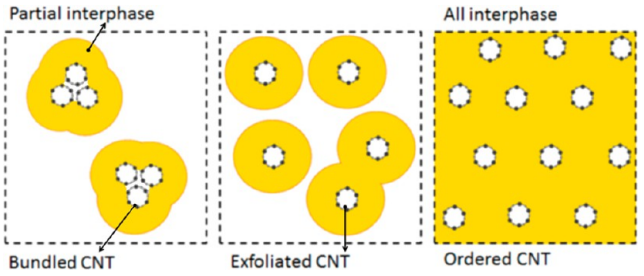

Figure 5. Illustration of interphase regions in CNT/polymer composites. Black circles represant CNTs, white regions represent bulk polymer matrix, and yellow regions represent highly ordered interphase regions.

shrinkage that is caused by cyclization reaction occurs at a temperature roughly higher than 200 °C. The addition of 1 wt % CNT not only reduced physical entropic shrinkage from 15 to 13 % after fibers were heated to 200 °C, but also significantly reduced chemical reaction shrinkage from 23 to 7% after fibers were heated to 350 °C in air.[50] The concept of how CNT restricts the fiber shrinkage and retains polymer orientation above T_g are shown in Figure 7C. In a composite fiber, interphase polymer is well aligned in the vicinity of CNT. When the temperature increased to above T_g, the shrinkage force due to entropic relaxation will be shared by CNTs which leads to smaller shrinkage. Moreover, the addition of CNTs in fibers has been observed to retain polymer chain orientation even at a temperature above polymer melting point. Anand et al. used WAXD to characterize the orientation of PET crystals in oriented PET and PET/CNT films before and after being heated to a temperature above melting.[34] The WAXD patterns of these samples are shown in Figure 7B. After heating the neat PET fully lost its orientation, whereas PET/CNT sample retained some orientation.[34] This demonstrates that aligned CNTs helped to retain PET chain orientation even at the melting temperature.

3.4. Effect on Electrical and Thermal Conductivities. The formation of percolation path of CNTs can lead to greatly improved electrical conductivity of polymer.[61−68] The CNTs in polymeric fibers are aligned along fiber axis matrix and will lead to an anisotropic electrical conductivity. For example, in an oriented PP/MWNT (5.3 wt %) tape, the ratio of electrical conductivity in longitudinal direction over transverse direction

dx.doi.org/10.1021/am405136s | ACS Appl. Mater. Interfaces 2014, 6, 6069−6087

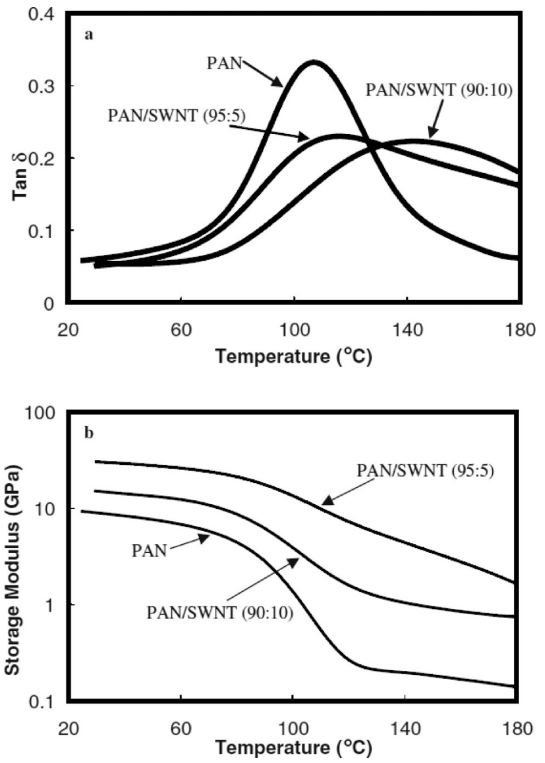

Figure 6. Dynamic mechanical (A) tan(δ) and (B) storage modulus as a function of temperature for PAN, PAN/SWNT (5 wt %), and PAN/SWNT (10 wt %) fibers. Reprinted with permission from ref 56. Copyright 2004 John Wiley.

increased from 1 for the isotropic film without stretching (electrical conductivity ~5 S/m) to 100 for the oriented film after tape was stretched in solid state to a draw ratio of 6 (longitudinal direction electrical conductivity ~0.07 S/m).[67] For electrical and thermal conductivity of CNT reinforced composite fibers, the conductivity is measured along the fiber axis, if not mentioned specifically. Although neat PEK is non-electrically conductive, PEK/FWNT (20 wt %) composite fiber, with a tensile strength of 0.12 GPa and tensile modulus of 17.3 GPa, has an axial electrical conductivity of 240 S/m.[69]

Polymeric fibers are anisotropic materials, and the CNTs orientation will affect the electrical conductivity of the composite fiber. Figure 8 shows possible effect of stretching on the dispersion and orientation of CNTs. Stretching of fibers can exfoliate CNT bundles (Figure 8, step A). However, the high degree of stretching may disrupt the formed CNT percolation network as shown in step B in Figure 8. There are contradicting observations on how the orientation of CNT affects composite fiber electrical conductivity. Rahul et al. observed that the electrical conductivity increased with increasing draw ratio of gel-spun CNT/polymeric fibers; for example, the electrical conductivity of PVA/SWNT (1 wt %) fiber increased from 1.52×10^{-4} to 6.13×10^{-3} S/m when total draw ratio increased from 8 to 42, and conductivity of 1 wt % MWNT/PAN fiber increased from 1.10×10^{-3} to 4.06×10^{-3} S/m when total draw ratio increased from 25 to 55.[62] Choi et al. also observed that if SWNT inside the epoxy-based composite was aligned under a strong magnetic field (25T) during curing, the conductivity increased by a factor of five, as compared to the unaligned sample. This increase was ascribed to the formation of a more efficient percolation pathway parallel to the magnetic field direction.[70] On the other hand, Du et al. observed that the electrical conductivity of PMMA/SWNT (2 wt %) fibers (~1×10^{-8} S/m) was 6 orders of magnitude lower than that of the isotropic composite (~1×10^{-2} S/m) at the same SWNT concentration.[71] Potschke et al. observed that the melt-spun PC/MWNT (2 wt %) fiber was non-conductive, whereas isotropic material was relatively conductive with a volume resistivity of 550 Ω cm (equal to 0.18 S/m) that is 15 orders of magnitude lower than neat PC fiber.[72] The significant decrease (up to several orders of magnitude) in electrical conductivity in drawn polymer/CNT fibers as compared with isotropic composite was also observed in PP&PE/CNT composite[47c] and PVA/MWNT composite.[52] The CNT percolation threshold in an isotropic composite normally is less than 0.1 wt % CNT[11] or even as low as 0.045 vol % for PVC/MWNT isotropic composite.[73] It is noted that the CNT percolation threshold would also depends on the CNT aspect ratio. In comparison, the reported CNT percolation thresholds in stretched polymer/CNT fibers were in the range of 0.5−2 wt % for PMMA/SWNT fiber[71,74] and ~1 wt % for PVA/MWNT.[75] The higher CNT percolation threshold concentration and lower electrical conductivity in polymer/CNT fibers as compared with isotropic composites are attributed to the CNT network disruption during fiber drawing. The electrical conductivity of a polymer/CNT fiber depends on the formation of CNT physical percolation network. The structures of CNT percolation network are affected by CNT length and diameter, and CNT dispersion status which vary in different composites. Thus the alignment of CNTs induced by the external force (such as fiber drawing) may increase or decrease the CNT percolation and thus may lead to increase or decrease in electrical conductivity for a specific composite system.

If a highly oriented polymer/CNT composite is annealed at a temperature higher than the glass-transition temperature, the relaxation of polymer chains will distort the orientation of aligned CNTs which could increase the chance of intertube contact and result in higher electrical conductivity (Figure 8, step C). Winey et al. measured the electrical conductivity of PMMA/SWNT composite, and observed that the percolation behavior depends on both the CNT loading and alignment.[74] At certain CNT loading, slight anisotropic distribution of CNT led to the best conductivity, whereas higher alignment of CNT reduced conductivity. Peijs et al. annealed highly oriented PP/MWNT (5.4 wt %) tape at 155 °C for 15 min and observed that the electrical conductivity of drawn and annealed sample (~90 S/m) was an order of magnitude higher than that of the isotropic sample (~9 S/m), which in turn was higher than that of the drawn sample prior to annealing (~0.07 S/m).[67] The increase in electrical conductivity after annealing is ascribed to the reconstructed CNT conductive networks caused by polymer relaxation during annealing. The increased electrical conductivity upon annealing was also observed for PP&PE/CNT (40, 60/0.42 wt %) bi-phase fibers, where the electrical conductivity decreased from 4 to 1.25 S/m when the draw ratio increased from 1 to 6, and then increased to 10 S/m after being annealed at 150 °C.[47c]

The addition of CNT in polymeric fiber is promising to enhance fiber's axis thermal conductivity, as individual CNTs have been reported to have high thermal conductivity in the range of 3000 to 6600 W m^{-1} K^{-1}.[76,77] The major issues hinder the improvement of thermal conductivity by incorporating CNTs in polymers are the high intertube and tube-polymer heat transfer resistances.[78] Unlike the significant improvement

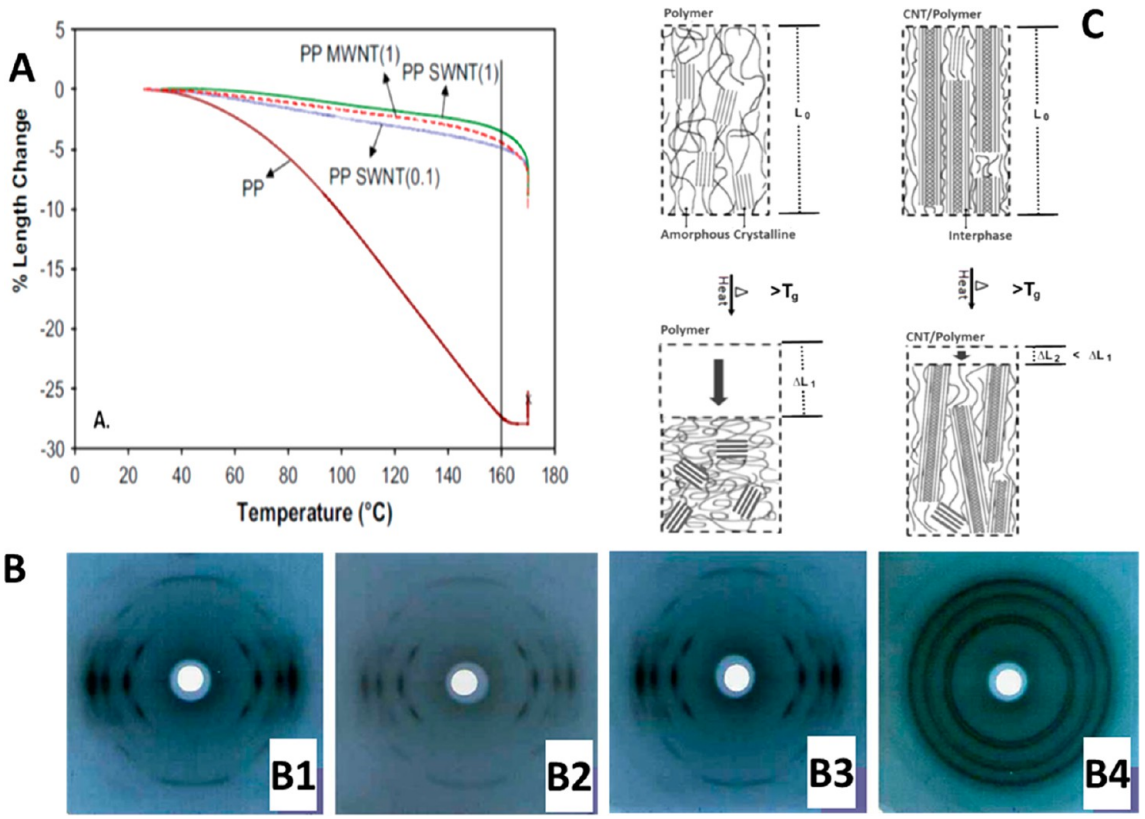

Figure 7. (A) Thermal shrinkage in PP fibers with and without CNTs (SWNT and MWNT) at various loadings. Reprinted with permission from ref 26. Copyright 2008 Elsevier. (B) WAXD patterns of (B1) PET/SWNT (1 wt %) nanocomposite after drawing, (B2) PET/SWNT (1 wt %) nanocomposite after melting and subsquent slow cooling at constant length, (B3) neat PET after drawing, (B4) neat drawn PET after melting and subsquent slow cooling at constant length. Reprinted with permission from ref 34. Copyright 2006 Elsevier. (C) Morphological change in oriented polymer and CNT/polymeric fibers when heated above the polymer glass-transition temperature. The two schematics on the left are polymer fibers without CNT. The two schematics on the right are polymeric fibers with CNT. The two schematics at the top are original drawn fibers, while the bottom two schematics are for fibers heated above the glass-transition temperature. Shrinkage in the control polymeric fiber is higher than the shrinkage in the composite fiber as a result of interaction between polymer and CNT.

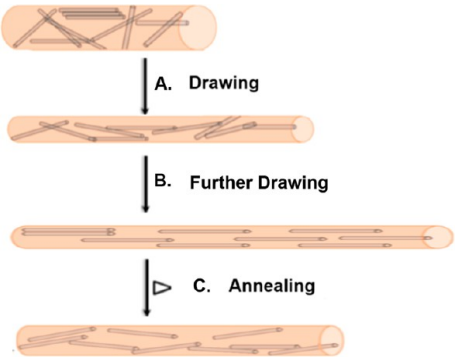

Figure 8. Schematics showing the possible effects of drawing and thermal annealing on the dispersion and orientation of CNT. (Step A) Drawing results in exfoliation of CNT bundles and better CNT orientation. (Step B) Very high CNT orientation can be achieved in highly drawn fiber. (Step C) Annealing above the glass-transition temperature can relax polymer molecules, and in turn can result in decreased CNT orientation. Thus, annealing can increase the probability of intertube contacts.

in electrical conductivity, incorporating CNTs in polymers only moderately improved thermal conductivity of the materials[79,80] such as electro-spun PAN/CNT fiber, and PVP/CNT fibers.[81] In comparison with isotropic composite, the enhancement of thermal conductivity in an anisotropic polymer/CNT fiber can be expected to be much higher, because the oriented structures of polymers and CNTs, as well as the formation of highly ordered interphase that will reduce the thermal resistance between CNTs and polymers, can improve thermal transport along fiber axis. In a recent study, the axial thermal conductivity of PEK fiber measured at room temperature increased from 0.5 to 5 to 10 to 15 W m^{-1} K^{-1} when MWNT loading increased from 5 to 10 to 20 to 28 wt %, respectively (Figure 9A).[82] Figure 9B shows the cross-sectional SEM images of PEK and PEK/CNT composite fibers. When CNT loading increased to 20 wt % or higher, the cross-section of composite fibers changed from solid to highly porous.[69]

Bicomponent fiber spinning can produce fibers with sheath–core, side-by-side, layer-by-layer, island-in-a-sea, and segmented pie geometries.[83] Incorporating CNTs in one component of a bicomponent fiber may extensively change its electrical and thermal conductivities to provide new functionality. Miyauchi et al. used coaxial electrospinning to spin cellulose (sheath)/MWNT (core) fibers with an electrical conductivity of 10.7 S/m at 45 wt % MWNT loading.[84] Longson et al. used coaxial electrospinning to spin PMMA (sheath)/MWNT (core) fibers[85] and Ojha et al. electro-spun PEO/MWNT (sheath)/PEO (core) nanofibers,[86] and they both observed that much higher electrical conductivity in bicomponent fibers than that in single-component mat at same MWNT loading. Chien et al. gel-spun PAN (sheath)/ PAN/MWNT (10 wt %) (core)

dx.doi.org/10.1021/am405136s | ACS Appl. Mater. Interfaces 2014, 6, 6069–6087

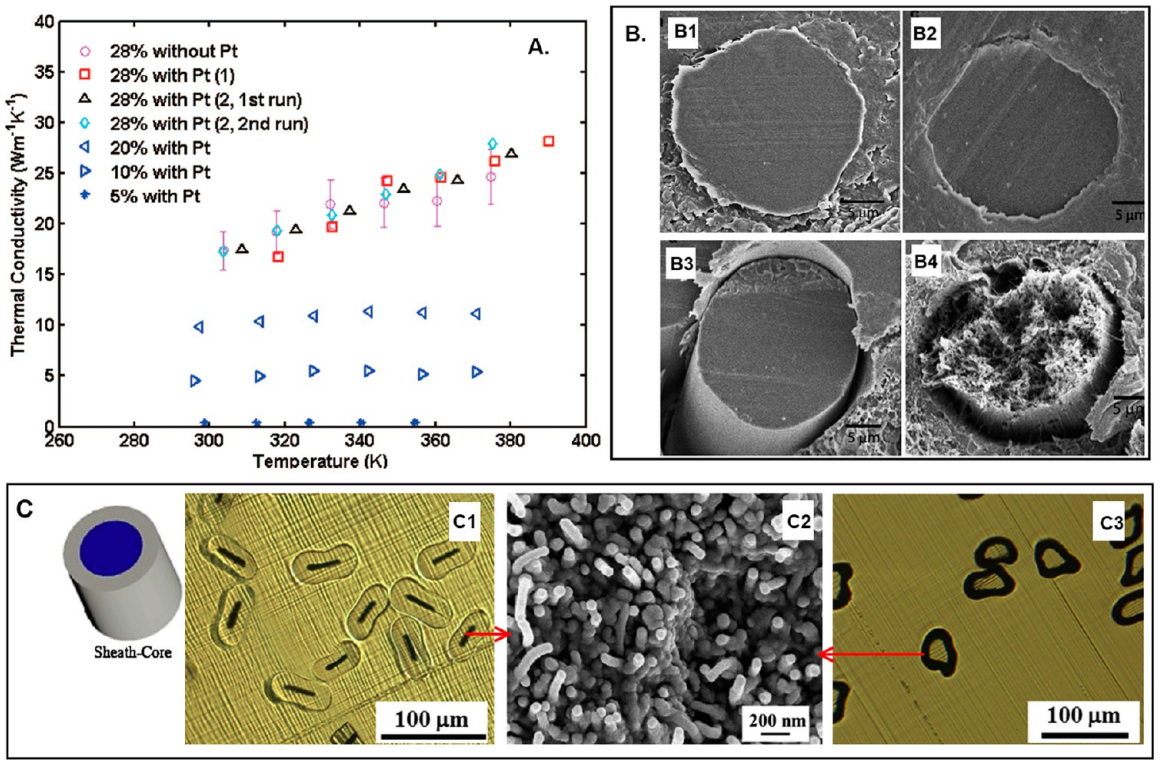

Figure 9. (A) Temperature-dependence of thermal conductivity in PEK/CNT fibers at CNT loadings of 5, 10, 20, and 28 wt %. Reprinted with permission from ref 82. Copyright 2012 American Institute of Physics. (B) Coss-section SEM images of various PEK/CNT fibers: (B1) PEK, (B2) PEK/CNT (5 wt %), (B3) PEK/CNT (10 wt %), and (B4) PEK/CNT (20 wt %). Reprinted with permission from ref 69. Copyright 2010 Elsevier. (C) Bicomponent fibers. Optical images of (C1) PAN sheath and PAN/MWNT (with 10 wt % MWNT) core and (C3) PAN/MWNT (10 wt % MWNT) sheath and PAN core bicomponent as-spun fibers. (C2) SEM image of tensile fracture section of the PAN/MWNT (10 wt %) portion in the drawn fibers. Reprinted with permission from ref 87. Copyright 2013 Elsevier.

bicomponent fibers which had tensile strength of 0.72 GPa and tensile modulus of 20 GPa. The components of the sheath and core were switchable. The optical cross-section images of the bicomponent fibers and SEM image of the fracture surface of composite portion are shown in Figure 9C. The bicomponent PAN (sheath)/composite (core) fiber had electrical conductivity of 1.49×10^{-5} S/m and thermal conductivity of 2.6 W m^{-1} K^{-1}, which increased to 0.366 S/m and thermal conductivity of 7 W m^{-1} K^{-1}, respectively, after annealing at 180 °C for 2 h.[87]

3.5. Enhanced Environmental Performance. CNTs containing polymeric fibers exhibit better resistance to environmental conditions, such as high temperature, organic solvents, and radiation, than neat polymeric fibers. Figure 10A shows TGA curves of PMMA and PMMA/SWNT composites. The maximum weight loss for composite occurred at 372 °C, which was 61 °C higher than that for pure PMMA.[71] With the addition of CNTs, improvement of polymer thermal stability has been observed in many systems, such as the on-set decomposition temperature of PP fiber was increased from 320 to 336 to 354 °C while CNT loading increased from 0 to 0.5 to 1 wt %, respectively.[88] The onset decomposition temperature for PVA fiber increased from 201 to 260 °C with the addition of 4.5 wt % MWNT,[89] increased from 274 to 313 °C for cellulose fiber with the addition of 9 wt % MWNT,[90] and from 270 to 320 °C for PMMA fiber with the addition of 5 wt % MWNT.[54] Additionally, CNT containing polymeric fibers have better chemical resistance to organic solvents.[42] Figure 10B shows optical images of PVA and PVA/SWNT fibers soaked in DMSO at various temperatures. At 60 °C, PVA/SWNT fiber was mostly intact, whereas PVA fiber had disintegrated into fibrils. At 85 °C, PVA fiber was fully dissolved, whereas PVA/SWNT fiber was swollen but intact. Sreekumar et al observed that solution-spun PAN/SWNT (10 wt %) composite fiber was insoluble in DMF at room temperature after several days, whereas PAN fiber is soluble.[42] Highly drawn gel-spun PAN fiber that was insoluble at room temperature DMF for days was dissolved in boiling DMF in a few minutes. In comparison, gel-spun PAN/SWNT (1 wt %) fibers only fragmented in boiling DMF even after 30 min.[36] The presence of CNTs in polymers was also found to enhance electron beam radiation resistance of PVA[40] and PAN.[39] Those composites' crystal lattices were able to be imaged by high resolution TEM at 200kv electron acceleration voltage, whereas neat polymer samples could not be imaged under comparable measurement conditions, as their shapes deformed and their crystalline structures turned into amorphous quickly under the comparable electron beam exposure.

3.6. Rheology of Polymer/CNT Composite Melts and Solutions. The rheology of a polymer system can be affected by the presence of CNTs. Figure 11A shows a polymer system with randomly oriented CNT bundles.[91] At relatively low CNT loadings, no CNT contacts are formed, and the rheological behavior of the composite is expected to be similar to the rheological behavior of the polymer without CNT (schematic on the left in Figure 11A). At a higher CNT concentration where the two adjacent CNTs are able connect the two polymer chains and thus form a network (schematic in the middle in Figure 11A), the rheological behavior changes while the system may remain electrically insulating. This concen-

dx.doi.org/10.1021/am405136s | ACS Appl. Mater. Interfaces 2014, 6, 6069−6087

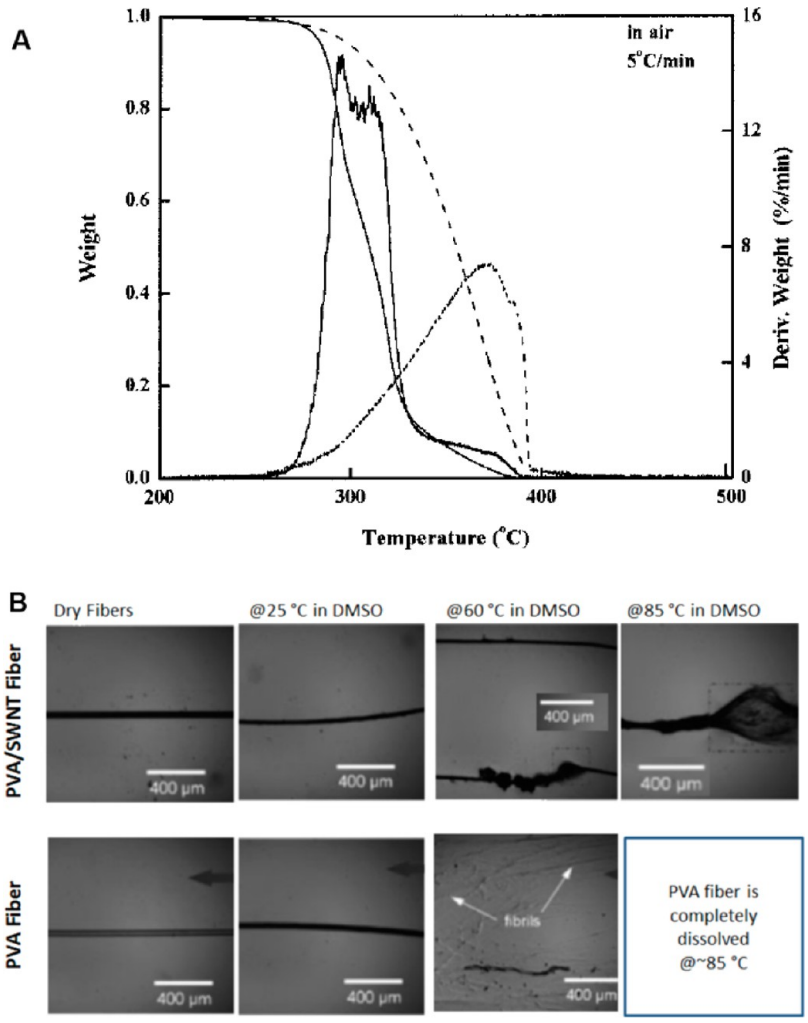

Figure 10. (A) Thermogravimetric analysis of the normalized weight loss for PMMA (solid line) and PMMA/SWNT (0.5 wt %) (dashed line) composite heated in air at 5 °C/min. Reprinted with permission from ref 71. Copyright 2003 John Wiley. (B) Optical micrographs of PVA and PVA/SWNT fibers after being soaked in DMSO at various temperatures for 30 min. Reprinted with permission from ref 42. Copyright 2009 John Wiley.

tration would be referred to having achieved rheological percolation. At even higher CNT concentration, where CNTs also make physical connection with each other or are within electron tunneling distance of each other, then system becomes electrically conducting (schematic on the right in Figure 11A). The studies show that the percolation threshold based on rheology and electrical conductivity was 0.12 and 0.39 wt %, respectively, for PMMA/SWNT composite,[91] and 0.6 and 0.9 wt %, respectively, for PET/MWNT composite.[92] It is noted that the percolation behavior would also depend on the CNT aspect ratio and processing conditions, among other factors.

The rheological behavior of polymer composite melt or solution under high shear rate is important for producing composite fibers, as relatively high shear rates (>1000 s^{-1}) are experienced during both melt and solution spinning. Abdel-Goad et al. measured rheology of PC/MWNT composite melt at 280 °C and observed that the complex viscosity increased when MWNT loading was higher than 0.5 wt % (rheology threshold). Also, the shear thinning exponent n ($|\eta^*| \approx \omega^{-n}$, where η^* is complex viscosity and ω is shear rate) determined at low shear rate region (between 0.056 and 0.56 rad/s) remarkably increased from 0.05 to 0.5 to 0.9 when MWNT loading increased from 0 to 0.5 to 1 wt %, respectively.[93] Wu et al. observed similar shear thinning rheological behavior for PBT/MWNT melt system. While the viscosity of pure PBT melt was insensitive over a long range of frequency (from 0.01 to 100 Hz), PBT/MWNT melt exhibited shear thinning when MWNT loading was higher than 2 wt %.[94]

Viscosity as a function of shear rate for PAN and PAN/CNF composite solutions in DMF is plotted in Figure 11B.[62] Although the viscosity of composite solution was higher than PAN solution at low shear rate (< 1 s^{-1}), the viscosity became lower at high shear rate (> 5 s^{-1}) because of more significant shear thinning caused by the addition of CNFs. Via et al. measured rheological properties of PC/MWNT melts at 270 °C using capillary rheometer and observed that the complex viscosity of PC/MWNT (at 6 wt % MWNT) melt decreased by a factor of 4 as compared to that of PC when shearing rate was at ~10 000 rad/s, whereas the viscosity of the composite melt was more than two orders of magnitude higher than PC at 1 rad/s.[95] The significant shear thinning induced by the addition of CNTs in polymer melts and solutions is expected to have significant impact on polymer processing.

3.7. Fatigue Behavior. If a material undergoes repeated loading and unloading, structural damage or fatigue will occur. Carey et al observed that poly(dimethylsiloxane)/MWNT

dx.doi.org/10.1021/am405136s | ACS Appl. Mater. Interfaces 2014, 6, 6069−6087

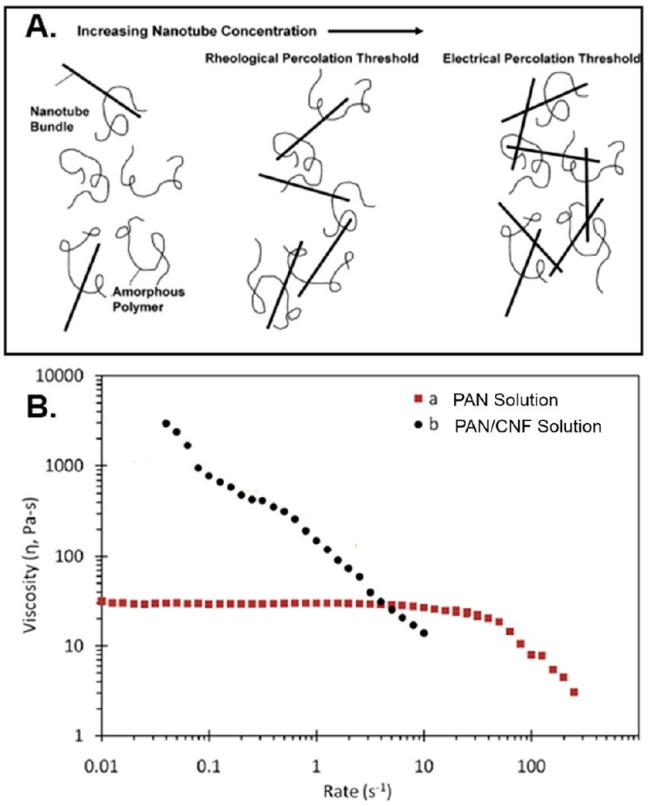

Figure 11. (A) Schematic of SWNT/polymer nanocomposites in which the nanotube bundles have isotropic orientation. (Left) At low nanotube concentrations, the rheological and electrical properties of the composite are comparable to those of the host polymer. (Middle) The onset of rheological percolation. (Right) The onset of electrical percolation. Reprinted with permission from ref 91. Copyright 2004 American Chemical Society. (B) Viscosity of PAN/DMF and PAN/CNF/DMF solutions as a function of shear rate. The concentration for both samples is 15 g solids per 100 ml of DMF. Sample is is only PAN and sample contains PAN/CNF ratio of 80/20. Reprinted with permission from ref 62. Copyright 2009 Georgia Institute of Technology.

(vertically aligned) nanocomposite exhibited a self-stiffening response under cyclic compressive loading which resulted in increased in stiffness.[96] Kuronuma et al. found that the addition of MWNT in PC matrix improved its fatigue crack growth resistance.[97] Loos et al. showed that the presence of CNTs in PU increased the fatigue life (at 50 MPa cyclic peak stress) by up to 248%.[98] The improved fatigue life by the addition of CNTs in polymer matrix was also found in CNT reinforced polymer fibers. Kolluru tested fatigue life of PAN and PAN/SWNT (containing 5 wt % SWNT) fibers at 40 Hz under a cyclic load (at 60% of the breaking load for the control PAN fiber).[99] It was found that PAN/SWNT composite fibers did not fail even after 25 million cycles, whereas the PAN fibers without CNT failed after 3.9 million cycles.

4. CNT REINFORCED HIGH-PERFORMANCE POLYMERIC FIBERS

On the basis of the search from Web of Science as of October 2013, more than 15 000 papers have been published on the topic of CNT-reinforced polymeric materials as determined by the following keywords search: "carbon nanotube" and "polymer" in topic, and more than 2400 papers are related to fibers by refining search results using "fiber". Rather than giving a comprehensive progress review on various polymer/CNT fibers, this section focuses on recent advances in CNT-reinforced polymer or polymer derived fibers with both high tensile strength and high tensile modulus.

4.1. PAN-Derived Carbon Fiber. Carbon fibers with high tensile properties are important reinforcing materials. High-performance carbon fiber is made by pyrolyzing PAN fiber. The structure of PAN precursor fiber affects the properties of the resultant carbon fiber. Incorporating CNT in precursor PAN fiber has been found to improve fiber tensile properties. Under identical gel-spinning conditions, addition of 1 wt % SWNT increased tensile strength and modulus of PAN fibers from 0.90 to 1.07 GPa and from 22.1 to 28.7 GPa, respectively.[49] PAN chains in the vicinity of CNTs are highly oriented and extended along CNTs' axis.[49,50] The interphase PAN can be developed

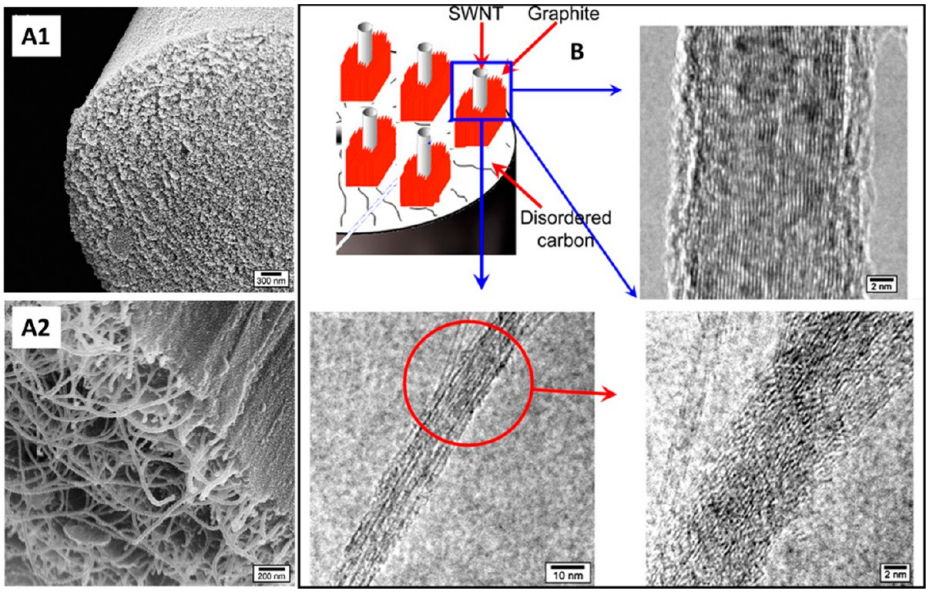

Figure 12. SEM micrographs of cross sections of carbonized (A1) PAN and (A2) PAN/SWNT (1 wt %) fibers. (B) HR-TEM images and schematic representation of carbonized PAN/SWNT (1 wt %) fibers. Reprinted with permission from ref 100. Copyright 2007 Elsevier.

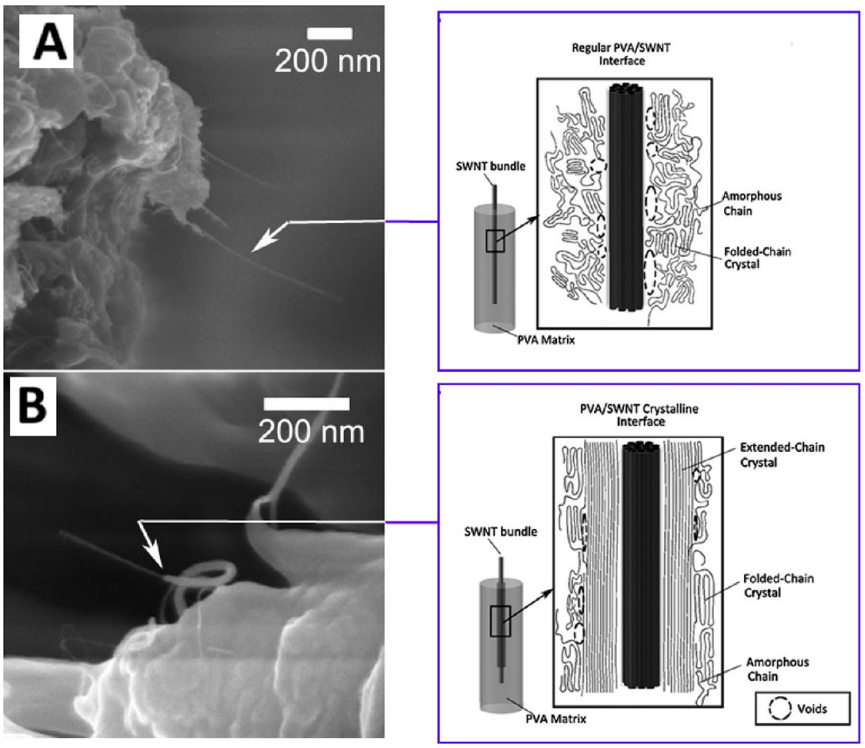

Figure 13. High-resolution SEM images of the fracture surface of (A) PVA/SWNT fiber with no interphase and (B) PVA/SWNT fiber showing the formation of the interphase layer. The schematics depicting PVA and SWNT bundles are shown on the right. Without the interfacial crystallization, the degree of contact between PVA and SWNT is not very high. Regions depicting dashed ovals indicate gaps between PVA and SWNT, as shown in the figure on the top right. The figure on the bottom right shows highly ordered interfacial crystallization PVA layer in the vicinity of CNT, providing high degree of contact between PVA and CNT. Reprinted with permission from ref 109. Copyright 2013 John Wiley.

into more perfect carbon structure than PAN matrix. Figure 12A shows SEM cross-section images of carbonized PAN and PAN/SWNT fibers. It can be observed that nano-fibrils were embedded in the brittle carbon matrix. These nano-fibrils are SWNT coated by well-developed graphitic layers as shown in Figure 12B. The Raman G band excitation of SWNT was found to be strongly quenched by the formation of graphitic layers. It was also found that the tensile strength and modulus of the carbonized fiber increased from 1.1 to 1.8 N/tex and from 168 to 250 N/tex, respectively, with the addition of 1 wt % CNT in PAN precursor fiber.[100] This improvement in carbon fiber tensile properties is due to the formation of more oriented and less defect carbon structures developed from the highly ordered interphase PAN layer observed in the vicinity of PAN/CNT precursor fibers.[49] TEM studies on in situ carbonization of electro-spun PAN/MWNT fibers at various elevated temperatures also verified that the addition of CNTs enhanced the formation and orientation of graphitic structure.[101,102] Additionally, Lanticse-Diaz et al. observed that the addition of MWNT could induce stress graphitization in glass-like carbon matrix that is a non-graphitizing material after carbonization at 1000 °C.[103] Papkov et al. observed that the addition of double walled CNT (1.2 wt %) in electro-spun PAN fiber significantly improved graphitic structure and orientation after carbonization, and the molecular dynamic simulation also confirmed the growth of oriented graphitic structure in the vicinity of CNTs.[104]

4.2. PVA Fiber. PVA crystal has a planar zig-zag chain conformation.[105] The theoretical modulus of a perfectly oriented PVA fiber is estimated to be in the range of 250−300 GPa. The commercial high strength and high modulus PVA fibers are mainly manufactured by Kuraray Co. Ltd. (Tokyo, Japan) with a tensile modulus and strength in the range of 11−43 GPa and 0.9−1.9 GPa, respectively. CNT was observed to nucleate and template the growth of PVA crystals during solution crystallization.[40−42] Zhang et al. found that the addition of 3 wt % CNT increased tensile strength and modulus of gel-spun PVA fibers from 0.9 to 1.1 GPa and from 25.6 to 35.8 GPa, respectively, when spun under the identical processing conditions.[106] Miaudet et al. incorporated 0.35 wt % SWNT in wet-spun PVA fiber and observed that tensile modulus and strength increased from 2.5 to 14.5 GPa and from 0.6 to 1.6 GPa, respectively.[107] Xu et al. incorporated 0.3 wt % SWNT in gel-spun PVA fibers and improved the tensile modulus and strength from 28 to 36 GPa and from 1.7 to 2.2 GPa, respectively.[108] After optimizing gel spinning and drawing conditions, Minus et al. found that the addition of 1 wt % SWNT in PVA fibers increased the tensile modulus and strength of PVA fiber from 48 to 71 GPa and from 1.6 to 2.6 GPa, respectively.[42]

In a recent PVA/SWNT fiber study, Minus et al. controlled shear and temperature conditions to induce PVA crystallization on SWNT at the composite solution preparation stage.[109] During PVA/SWNT solution preparation, the temperature of hot plate was increased to 160 °C in the first 2 h and then subsequently cooled to 120 °C to induce PVA crystallizations. In the control composite solution preparation, the hot plate temperature was maintained at 120 °C. Images A and B in Figure 13 show SEM images of fracture surfaces for PVA/SWNT (10 wt %) fibers.[109] A 8.2 nm thick PVA interphase layer was observed on 10.3 nm SWNT bundles in a PVA/SWNT sample that went through a temperature induced

crystallization protocol. The PVA/SWNT fiber using above PVA crystallized CNTs showed tensile strength, modulus and toughness of 4.9 GPa, 128 GPa, and 202 J/g, respectively. In comparison, without this protocol, no PVA coating layer was observed on the SWNT bundle surface, and the tensile strength, modulus and toughness of the resulting PVA/SWNT fibers were 2.5 GPa, 36 GPa, and 101 J/g, respectively. This study clearly shows the importance of the interphase formation and its effect on tensile properties of the composite fiber.

4.3. Rigid-Rod Polymeric Fibers. Rigid-rod polymers that have much better high temperature resistance than flexible chain polymers are classified into lyotropic and thermotropic liquid crystalline polymers (TLCP).[110] Vectra (thermotropic LC), Zylon (PBO, lyotropic LC), and Kevlar (poly(*p*-phenylene terepthalamide), PPTA, lyotropic LC) are examples of successful commercial rigid-rod polymeric fibers. The CNT dispersed in LC phases has been observed to be well-aligned along the direction of LC region. Figure 14A shows polarized Raman spectra of SWNT in a chiral nematic lyotropic LC phase.[111] The SWCNT Raman intensity at the polarization angle perpendicular to the helix axis was considerably stronger than that at the parallel angle. Since LC director was perpendicular to the helix axis, above results confirmed that SWNTs were aligned along the LC director. Same observation was also found in a SWNT/5CB (4-Cyano-4′-pentylbiphenyl) LC system.[112,113] When CNTs are aligned along the LC director, the system's free energy is minimized under this status. While the orientation of CNTs in LC is not an issue, researches focus on the possible benefits by incorporating CNTs into LC fibers. Tang et al. blended 1 wt % MWNTs into TLCP (Vectra) and found that the tensile strength and modulus of fiber increased from 0.87 to 1.17 GPa and from 81 to 111 GPa, respectively.[114] Kumar et al. synthesized PBO with the presence of SWNT in poly(phosphoric acid), and then spun the solution into fiber by dry-jet wet-spinning.[115] Incorporating 10 wt % SWNT in PBO fibers increased the tensile modulus and strength from 138 to 167 GPa and from 2.6 to 4.2 GPa, respectively. Kim et al. synthesized PPTA/CNT composite by in situ polymerization in N-methyl pyrolidone and observed enhanced electrical conductivity in the composite, but did not spin the composite dope into fiber form.[116] Sainsbury et al. functionalized MWNT by PPTA and observed better dispersion with PPTA than unmodified MWNT.[117] Fuming sulfuric acid (H_2SO_4), which may also dissolve PPTA, has been shown to protonate SWNT and exfoliate SWNT bundles and ropes.[4] Davis et al. observed different phases for SWNTs dissolved in super-acid (102% H_2SO_4).[118] At low concentration (< 4 vol %), the solution was isotropic, at intermediate concentration (4−5 vol %), it formed a single nematic phase, whereas above >5 vol % concentration, polydomain nematic liquid crystal was reported. The phase of CNTs in super-acid affects its rheological behavior, as expected (Figure 14B).

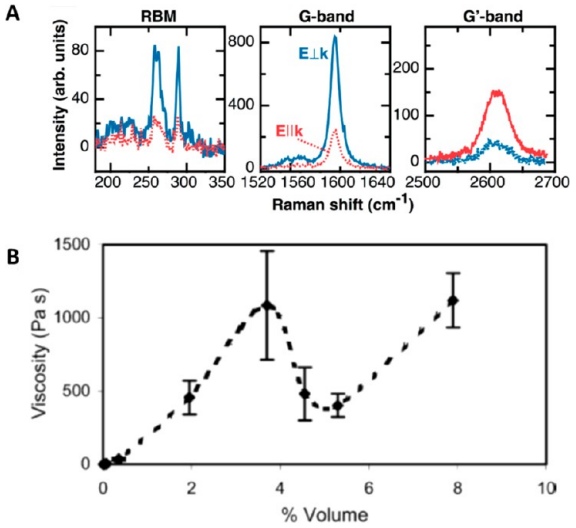

Figure 14. (A) Three characteristic SWNT Raman bands in the polarized resonant Raman spectra obtained on SWNT containing (0.03 mg/mL SWNTs) chiral nematic LC sample with light polarization perpendicular (blue) and parallel (red) to the LC helix axis, respectively. Reprinted with permission from ref 111. Copyright 2007 John Wiley.(B) Viscosity as a function of SWNT concentration in 102% H_2SO_4 at a shear rate of 0.1 s^{-1}. Reprinted with permission from ref 118. Copyright 2013 American Chemical Society.

Yutong et al. studied the rheology of blended PPTA/H_2SO_4 (19.5 wt %) solution with weight fractions of SWNT in the range from 0 to 0.6 wt % (based on the weight of H_2SO_4).[119] The complex viscosity was reduced from 9 × 10^5 Pa·s at 0% SWNT to 4 × 10^5 Pa.s at 0.2 wt % SWNT measured at the shear rate of 1 s^{-1} at 80 °C, and then increased monotonously when CNT concentration increased from 0.2 to 0.6 wt %. Deng et al. characterized PPTA and PPTA/SWNT fibers and found that CNT orientation was lower than PPTA chains which led to lower orientation of PPTA chains in the composite fibers.[120] The given stress−strain curves suggest that reinforcement of SWNT only occurs at a low draw ratio of 2, the properties of PPTA/SWNT fiber are weaker than control PPTA fiber at a draw ratio higher than 4. However, the dope preparation and spinning conditions are not given. Instead of mixing CNT with polymer and spinning into fiber, O'Connor et al. made PPTA/CNT fibers by swelling Kevlar in nanotube suspensions. With 1 wt % CNT absorption by Kevlar, the strength increased from 3.9 to 4.8 GPa and modulus moderately increased from 120 to 130 GPa.[121]

4. CONCLUSIONS

This review summarizes processing conditions of CNT reinforced polymeric fibers and their structure and properties. Many studies report that the incorporation of CNTs reinforces the tensile properties for many polymeric fibers, such as PE, PP, PVA, PC, PMMA, PVA, PAN, PBO, PAni, cellulose, PBO, and PPTA. During processing, polymer−CNT interaction can lead to the formation of the interphase layer, where the polymer is more ordered, more crystalline, and better oriented than the rest of the polymer in the fiber. The interphase polymer is important for the fiber performance, as it not only can improve the stress transfer between the rest of the polymer matrix and the CNTs to fully utilize the exceptional tensile properties of CNTs, but also can enhance the fiber properties, as the highly ordered interphase layer itself will have much better mechanical properties than rest of the polymer matrix. CNT type, CNT dispersion status, interaction between polymer and CNT, and orientation of polymer chains and CNTs are key factors for determining the performance of a polymer-based composite fiber. Comprehensive understanding of these factors, especially the microstructure development and property characterization of the interphase polymer, are highly desired but still remain as key challenges for nanocomposite fiber processing. Moreover, the addition of CNTs in polymeric fibers also promotes other functionalities, such as electrical and thermal conductivities. By

manipulating CNT type, CNT concentration, and processing conditions, it is possible to tailor their electrical and thermal conductivities, while still achieving good mechanical properties.

AUTHOR INFORMATION

Corresponding Author

*E-mail: satish.kumar@mse.gatech.edu. Tel: +1 404 894-7550. Fax: +1 404 894-8780.

Notes

The authors declare no competing financial interest.

ACKNOWLEDGMENTS

Funding from DARPA and Army Research Office (grant number W911NF-10-1-0098) is gratefully acknowledged.

REFERENCES

(1) Hearle, J. W. S., *High-Performance Fibres*; Woodhead Publishing: Cambridge, U.K., 2001; pp 2−16.
(2) Iijima, S. *Nature* **1991**, *354* (6348), 56−58.
(3) Vigolo, B.; Pénicaud, A.; Coulon, C.; Sauder, C.; Pailler, R.; Journet, C.; Bernier, P.; Poulin, P. *Science* **2000**, *290* (5495), 1331−1334.
(4) Ericson, L. M.; Fan, H.; Peng, H.; Davis, V. A.; Zhou, W.; Sulpizio, J.; Wang, Y.; Booker, R.; Vavro, J.; Guthy, C.; Parra-Vasquez, A. N. G.; Kim, M. J.; Ramesh, S.; Saini, R. K.; Kittrell, C.; Lavin, G.; Schmidt, H.; Adams, W. W.; Billups, W. E.; Pasquali, M.; Hwang, W.-F.; Hauge, R. H.; Fischer, J. E.; Smalley, R. E. *Science* **2004**, *305* (5689), 1447−1450.
(5) Zhang, M.; Atkinson, K. R.; Baughman, R. H. *Science* **2004**, *306* (5700), 1358−1361.
(6) Li, Y.; Kinloch, I. A.; Windle, A. H. *Science* **2004**, *304* (5668), 276−278.
(7) Koziol, K.; Vilatela, J.; Moisala, A.; Motta, M.; Cunniff, P.; Sennett, M.; Windle, A. *Science* **2007**, *318* (5858), 1892−1895.
(8) Cornwell, C. F.; Welch, C. R. *J. Chem. Phys.* **2011**, *134* (20), 204708.
(9) Ciselli, P.; Wang, Z.; Peijs, T. *Mater. Technol.* **2007**, *22* (1), 10−21.
(10) Coleman, J. N.; Khan, U.; Blau, W. J.; Gun'ko, Y. K. *Carbon* **2006**, *44* (9), 1624−1652.
(11) Spitalsky, Z.; Tasis, D.; Papagelis, K.; Galiotis, C. *Prog. Polym. Sci.* **2010**, *35* (3), 357−401.
(12) Thostenson, E. T.; Ren, Z.; Chou, T.-W. *Compos. Sci. Technol.* **2001**, *61* (13), 1899−1912.
(13) Moniruzzaman, M.; Winey, K. I. *Macromolecules* **2006**, *39* (16), 5194−5205.
(14) Loos, M. R.; Schulte, K. *Macromol. Theory Simul.* **2011**, *20* (5), 350−362.
(15) Grady, B. P. *Macromol. Rapid Commun.* **2010**, *31* (3), 247−257.
(16) Salvetat, J.-P.; Briggs, G. A. D.; Bonard, J.-M.; Bacsa, R. R.; Kulik, A. J.; Stöckli, T.; Burnham, N. A.; Forró, L. *Phys. Rev. Lett.* **1999**, *82* (5), 944−947.
(17) Basu-Dutt, S.; Minus, M. L.; Jain, R.; Nepal, D.; Kumar, S. *J. Chem. Educ.* **2012**, *89*, 221−229.
(18) Peigney, A.; Laurent, C.; Flahaut, E.; Bacsa, R. R.; Rousset, A. *Carbon* **2001**, *39* (4), 507−514.
(19) Cadek, M.; Coleman, J. N.; Ryan, K. P.; Nicolosi, V.; Bister, G.; Fonseca, A.; Nagy, J. B.; Szostak, K.; Béguin, F.; Blau, W. J. *Nano Lett.* **2004**, *4* (2), 353−356.
(20) Ramesh, S.; Ericson, L. M.; Davis, V. A.; Saini, R. K.; Kittrell, C.; Pasquali, M.; Billups, W. E.; Adams, W. W.; Hauge, R. H.; Smalley, R. E. *J. Phys. Chem. B* **2004**, *108* (26), 8794−8798.
(21) Parra-Vasquez, A. N. G.; Behabtu, N.; Green, M. J.; Pint, C. L.; Young, C. C.; Schmidt, J.; Kesselman, E.; Goyal, A.; Ajayan, P. M.; Cohen, Y.; Talmon, Y.; Hauge, R. H.; Pasquali, M. *ACS Nano* **2010**, *4* (7), 3969−3978.
(22) Pénicaud, A.; Poulin, P.; Derré, A.; Anglaret, E.; Petit, P. *J. Am. Chem. Soc.* **2004**, *127* (1), 8−9.
(23) Fukushima, T.; Aida, T. *Chem.—Eur. J.* **2007**, *13* (18), 5048−5058.
(24) Luo, S.; Liu, T.; Wang, B. *Carbon* **2010**, *48* (10), 2992−2994.
(25) Song, K. A.; Zhang, Y. Y.; Meng, J. S.; Green, E. C.; Tajaddod, N.; Li, H.; Minus, M. L. *Materials* **2013**, *6* (6), 2543−2577.
(26) Lee, G.-W.; Jagannathan, S.; Chae, H. G.; Minus, M. L.; Kumar, S. *Polymer* **2008**, *49* (7), 1831−1840.
(27) Sandler, J.; Broza, G.; Nolte, M.; Schulte, K.; Lam, Y. M.; Shaffer, M. S. P. *J. Macromol. Sci. Part B Phys.* **2003**, *42* (3-4), 479−488.
(28) Bhattacharyya, A. R.; Sreekumar, T. V.; Liu, T.; Kumar, S.; Ericson, L. M.; Hauge, R. H.; Smalley, R. E. *Polymer* **2003**, *44* (8), 2373−2377.
(29) Grady, B. P.; Pompeo, F.; Shambaugh, R. L.; Resasco, D. E. *J. Phys. Chem. B* **2002**, *106* (23), 5852−5858.
(30) Probst, O.; Moore, E. M.; Resasco, D. E.; Grady, B. P. *Polymer* **2004**, *45* (13), 4437−4443.
(31) Sandler, J. K. W.; Pegel, S.; Cadek, M.; Gojny, F.; van Es, M.; Lohmar, J.; Blau, W. J.; Schulte, K.; Windle, A. H.; Shaffer, M. S. P. *Polymer* **2004**, *45* (6), 2001−2015.
(32) Haggenmueller, R.; Fischer, J. E.; Winey, K. I. *Macromolecules* **2006**, *39* (8), 2964−2971.
(33) Anand, K. A.; Jose, T. S.; Agarwal, U. S.; Sreekumar, T. V.; Banwari, B.; Joseph, R. *Int. J. Polym. Mater.* **2010**, *59* (6), 438−449.
(34) Anand, K. A.; Agarwal, U. S.; Joseph, R. *Polymer* **2006**, *47* (11), 3976−3980.
(35) Zhang, S.; Kumar, S. *Macromol. Rapid Commun.* **2008**, *29* (7), 557−561.
(36) Li, L.; Li, C. Y.; Ni, C. *J. Am. Chem. Soc.* **2006**, *128* (5), 1692−1699.
(37) Zhang, S.; Lin, W.; Wong, C.; Bucknall, D. G.; Kumar, S. *ACS Appl. Mater. Interfaces* **2010**, *2* (6), 1642−1647.
(38) Mai, F.; Wang, K.; Yao, M.; Deng, H.; Chen, F.; Fu, Q. *J. Phys. Chem. B* **2010**, *114* (33), 10693−10702.
(39) Zhang, S.; Minus, M. L.; Zhu, L.; Wong, C.-P.; Kumar, S. *Polymer* **2008**, *49* (5), 1356−1364.
(40) Minus, M. L.; Chae, H. G.; Kumar, S. *Polymer* **2006**, *47* (11), 3705−3710.
(41) Minus, M. L.; Chae, H. G.; Kumar, S. *Macromol. Rapid Commun.* **2010**, *31* (3), 310−316.
(42) Minus, M. L.; Chae, H. G.; Kumar, S. *Macromol. Chem. Phys.* **2009**, *210* (21), 1799−1808.
(43) Voigt, W. *Annalen der Physik* **1889**, *274* (12), 573−587.
(44) Cox, H. L. *Br. J. Appl. Phys.* **1952**, *3* (3), 72.
(45) Fu, S.-Y.; Lauke, B. *Compos. Sci. Technol.* **1996**, *56* (10), 1179−1190.
(46) Liu, T.; Kumar, S. *Nano Lett.* **2003**, *3* (5), 647−650.
(47) Ding, W.; Eitan, A.; Fisher, F. T.; Chen, X.; Dikin, D. A.; Andrews, R.; Brinson, L. C.; Schadler, L. S.; Ruoff, R. S. *Nano Lett.* **2003**, *3* (11), 1593−1597.
(48) Barber, A. H.; Cohen, S. R.; Wagner, H. D. *Appl. Phys. Lett.* **2003**, *82* (23), 4140−4142.
(49) Chae, H. G.; Minus, M. L.; Kumar, S. *Polymer* **2006**, *47* (10), 3494−3504.
(50) Liu, Y.; Chae, H. G.; Kumar, S. *Carbon* **2011**, *49* (13), 4466−4476.
(51) Chae, H. G.; Kumar, S. *Science* **2008**, *319* (5865), 908−909.
(52) Chae, H. G.; Sreekumar, T. V.; Uchida, T.; Kumar, S. *Polymer* **2005**, *46* (24), 10925−10935.
(53) Jain, R.; Minus, M. L.; Chae, H. G.; Kumar, S. *Macromol. Mater. Eng.* **2010**, *295* (8), 742−749.
(54) Zeng, J.; Saltysiak, B.; Johnson, W. S.; Schiraldi, D. A.; Kumar, S. *Composites, Part B* **2004**, *35* (2), 173−178.
(55) Mazinani, S.; Ajji, A.; Dubois, C. *Polym. Eng. Sci.* **2010**, *50* (10), 1956−1968.
(56) Sreekumar, T. V.; Liu, T.; Min, B. G.; Guo, H.; Kumar, S.; Hauge, R. H.; Smalley, R. E. *Adv. Mater.* **2004**, *16* (1), 58−61.

(57) Baji, A.; Mai, Y.; Wong, S.; Abtahi, M.; Du, X. *Compos. Sci. Technol.* **2010**, *70* (9), 1401−1409.
(58) Yeh, J.; Lai, Y.; Liu, H.; Shu, Y.; Huang, C.; Huang, K.; Chen, K. *Polym. Int.* **2011**, *60* (1), 59−68.
(59) Rahatekar, S. S.; Rasheed, A.; Jain, R.; Zammarano, M.; Koziol, K. K.; Windle, A. H.; Gilman, J. W.; Kumar, S. *Polymer* **2009**, *50* (19), 4577−4583.
(60) Hou, H.; Ge, J. J.; Zeng, J.; Li, Q.; Reneker, D. H.; Greiner, A.; Cheng, S. Z. D. *Chem. Mater.* **2005**, *17* (5), 967−973.
(61) Mottaghitalab, V.; Spinks, G. M.; Wallace, G. G. *Synth. Met.* **2005**, *152* (1-3), 77−80.
(62) Jain, R. Carbon nanotube reinforced polyacrylonitrile and poly(etherketone) fibers. *PhD Thesis*, Georgia Institute of Technology, Atlanta, GA, 2009.
(63) Gao, X.; Zhang, S.; Mai, F.; Lin, L.; Deng, Y.; Deng, H.; Fu, Q. *J. Mater. Chem.* **2011**, *21* (17), 6401−6408.
(64) Soroudi, A.; Skrifvars, M. *Synth. Met.* **2010**, *160* (11-12), 1143−1147.
(65) Liu, K.; Sun, Y.; Lin, X.; Zhou, R.; Wang, J.; Fan, S.; Jiang, K. *ACS Nano* **2010**, *4* (10), 5827−5834.
(66) Bilotti, E.; Zhang, R.; Deng, H.; Baxendale, M.; Peijs, T. *J. Mater. Chem.* **2010**, *20* (42), 9449−9455.
(67) Deng, H.; Zhang, R.; Reynolds, C. T.; Bilotti, E.; Peijs, T. *Macromol. Mater. Eng.* **2009**, *294* (11), 749−755.
(68) Xue, P.; Park, K. H.; Tao, X. M.; Chen, W.; Cheng, X. Y. *Composite Structures* **2007**, *78* (2), 271−277.
(69) Jain, R.; Choi, Y. H.; Liu, Y.; Minus, M. L.; Chae, H. G.; Kumar, S.; Baek, J.-B. *Polymer* **2010**, *51* (17), 3940−3947.
(70) Choi, E. *J. Appl. Phys.* **2003**, *94* (9), 6034.
(71) Du, F.; Fischer, J. E.; Winey, K. I. *J. Polym. Sci., Part B: Polym. Phys.* **2003**, *41* (24), 3333−3338.
(72) Pötschke, P.; Brünig, H.; Janke, A.; Fischer, D.; Jehnichen, D. *Polymer* **2005**, *46* (23), 10355−10363.
(73) Mamunya, Y.; Boudenne, A.; Lebovka, N.; Ibos, L.; Candau, Y.; Lisunova, M. *Compos. Sci. Technol.* **2008**, *68* (9), 1981−1988.
(74) Du, F.; Fischer, J. E.; Winey, K. I. *Phys. Rev. B: Condens. Matter Mater. Phys.* **2005**, *72* (12), 121404.
(75) Bin, Y.; Mine, M.; Koganemaru, A.; Jiang, X.; Matsuo, M. *Polymer* **2006**, *47* (4), 1308−1317.
(76) Berber, S.; Kwon, Y.-K.; Tománek, D. *Phys. Rev. Lett.* **2000**, *84* (20), 4613.
(77) Kim, P.; Shi, L.; Majumdar, A.; McEuen, P. L. *Phys. Rev. Lett.* **2001**, *87* (21), 215502.
(78) Han, Z.; Fina, A. *Prog. Polym. Sci.* **2011**, *36* (7), 914−944.
(79) Moisala, A.; Li, Q.; Kinloch, I. A.; Windle, A. H. *Compos. Sci. Technol.* **2006**, *66* (10), 1285−1288.
(80) Gojny, F. H.; Wichmann, M. H. G.; Fiedler, B.; Kinloch, I. A.; Bauhofer, W.; Windle, A. H.; Schulte, K. *Polymer* **2006**, *47* (6), 2036−2045.
(81) Khan, W. S.; Asmatulu, R.; Ahmed, I.; Ravigururajan, T. S. *Int. J. Therm. Sci.* **2013**, *71* (0), 74−79.
(82) Moon, J.; Weaver, K.; Feng, B.; Gi Chae, H.; Kumar, S.; Baek, J.-B.; Peterson, G. P. *Rev. Sci. Instrum.* **2012**, *83* (1), 016103.
(83) Cooke, T. F. *Bicomponent Fibers: A Review of the Literature*. TRI: Princeton, NJ, 1993; pp 1−66.
(84) Miyauchi, M.; Miao, J.; Simmons, T. J.; Lee, J.-W.; Doherty, T. V.; Dordick, J. S.; Linhardt, R. J. *Biomacromolecules* **2010**, *11* (9), 2440−2445.
(85) Longson, T. J.; Bhowmick, R.; Gu, C.; Cruden, B. A. *J. Phys. Chem. C* **2011**, *115* (26), 12742−12750.
(86) Ojha, S. S.; Stevens, D. R.; Stano, K.; Hoffman, T.; Clarke, L. I.; Gorga, R. E. *Macromolecules* **2008**, *41* (7), 2509−2513.
(87) Chien, A.; Gulgunje, P. V.; Chae, H. G.; Joshi, A. S.; Moon, J.; Feng, B.; Peterson, G. P.; Kumar, S. *Polymer* **2013**, *54* (22), 6210−6217.
(88) Jose, M. V.; Dean, D.; Tyner, J.; Price, G.; Nyairo, E. *J. Appl. Polym. Sci.* **2007**, *103* (6), 3844−3850.
(89) Minoo, N.; Lin, T.; Tian, W.; Dai, L.; Wang, X. *Nanotechnology* **2007**, *18* (22), 225605.
(90) Zhang, H.; Wang, Z. G.; Zhang, Z. N.; Wu, J.; Zhang, J.; He, J. S. *Adv. Mater.* **2007**, *19* (5), 698−704.
(91) Du, F.; Scogna, R. C.; Zhou, W.; Brand, S.; Fischer, J. E.; Winey, K. I. *Macromolecules* **2004**, *37* (24), 9048−9055.
(92) Devasia, R.; Nair, C. P. R.; Sadhana, R.; Babu, N. S.; Ninan, K. N. *J. Appl. Polym. Sci.* **2006**, *100* (4), 3055−3062.
(93) Abdel-Goad, M.; Pötschke, P. *J. Non-Newtonian Fluid Mech.* **2005**, *128* (1), 2−6.
(94) Wu, D.; Wu, L.; Zhang, M. *J. Polym. Sci., Part B: Polym. Phys.* **2007**, *45* (16), 2239−2251.
(95) Via, M. D.; Morrison, F. A.; King, J. A.; Caspary, J. A.; Mills, O. P.; Bogucki, G. R. *J. Appl. Polym. Sci.* **2011**, *121* (2), 1040−1051.
(96) Carey, B. J.; Patra, P. K.; Ci, L.; Silva, G. G.; Ajayan, P. M. *ACS Nano* **2011**, *5* (4), 2715−2722.
(97) Kuronuma, Y.; Shindo, Y.; Takeda, T.; Narita, F. *Eng. Fract. Mech.* **2011**, *78* (17), 3102−3110.
(98) Loos, M. R.; Yang, J.; Feke, D. L.; Manas-Zloczower, I.; Unal, S.; Younes, U. *Composites, Part B* **2013**, *44* (1), 740−744.
(99) Kolluru, C.; Kumar, S., *To be published*.
(100) Chae, H. G.; Minus, M. L.; Rasheed, A.; Kumar, S. *Polymer* **2007**, *48* (13), 3781−3789.
(101) Prilutsky, S.; Zussman, E.; Cohen, Y. *J. Polym. Sci., Part B: Polym. Phys.* **2010**, *48* (20), 2121−2128.
(102) Sabina, P.; Eyal, Z.; Yachin, C. *Nanotechnology* **2008**, *19* (16), 165603.
(103) Lanticse-Diaz, L. J.; Tanabe, Y.; Enami, T.; Nakamura, K.; Endo, M.; Yasuda, E. *Carbon* **2009**, *47* (4), 974−980.
(104) Papkov, D.; Beese, A. M.; Goponenko, A.; Zou, Y.; Naraghi, M.; Espinosa, H. D.; Saha, B.; Schatz, G. C.; Moravsky, A.; Loutfy, R.; Nguyen, S. T.; Dzenis, Y. *ACS Nano* **2012**, *7* (1), 126−142.
(105) Bunn, C. W. *Nature* **1948**, *161* (4102), 929−930.
(106) Zhang, X.; Liu, T.; Sreekumar, T. V.; Kumar, S.; Hu, X.; Smith, K. *Polymer* **2004**, *45* (26), 8801−8807.
(107) Miaudet, P.; Badaire, S.; Maugey, M.; Derre, A.; Pichot, V.; Launois, P.; Poulin, P.; Zakri, C. *Nano Lett.* **2005**, *5* (11), 2212−2215.
(108) Xu, X.; Uddin, A. J.; Aoki, K.; Gotoh, Y.; Saito, T.; Yumura, M. *Carbon* **2010**, *48* (7), 1977−1984.
(109) Meng, J.; Zhang, Y.; Song, K.; Minus, M. L. *Macromol. Mater. Eng.* **2013**, *299* (2), 144−153.
(110) Chae, H. G.; Kumar, S. *J. Appl. Polym. Sci.* **2006**, *100* (1), 791−802.
(111) Lagerwall, J.; Scalia, G.; Haluska, M.; Dettlaff-Weglikowska, U.; Roth, S.; Giesselmann, F. *Adv. Mater.* **2007**, *19* (3), 359−364.
(112) Lagerwall, J. P. F.; Scalia, G. *J. Mater. Chem.* **2008**, *18* (25), 2890−2898.
(113) Lynch, M. D.; Patrick, D. L. *Nano Lett.* **2002**, *2* (11), 1197−1201.
(114) Tang, Y.; Fang, L.; Gao, P. *J. Mater. Sci.* **2012**, *47* (23), 8094−8102.
(115) Kumar, S.; Dang, T. D.; Arnold, F. E.; Bhattacharyya, A. R.; Min, B. G.; Zhang, X.; Vaia, R. A.; Park, C.; Adams, W. W.; Hauge, R. H.; Smalley, R. E.; Ramesh, S.; Willis, P. A. *Macromolecules* **2002**, *35* (24), 9039−9043.
(116) Hun-Sik, K.; Seung Jun, M.; Rira, J.; Hyoung-Joon, J. *Mol. Cryst. Liquid Cryst.* **2008**, *492* (1), 20−27.
(117) Sainsbury, T.; Erickson, K.; Okawa, D.; Zonte, C. S.; Fréchet, J. M. J.; Zettl, A. *Chem. Mater.* **2010**, *22* (6), 2164−2171.
(118) Davis, V. A.; Ericson, L. M.; Parra-Vasquez, A. N. G.; Fan, H.; Wang, Y.; Prieto, V.; Longoria, J. A.; Ramesh, S.; Saini, R. K.; Kittrell, C.; Billups, W. E.; Adams, W. W.; Hauge, R. H.; Smalley, R. E.; Pasquali, M. *Macromolecules* **2003**, *37* (1), 154−160.
(119) Yutong, C.; Zhaofeng, L.; Xianghua, G.; Junrong, Y.; Zuming, H.; Ziqi, L. *Int. J. Mol. Sci.* **2010**, *11* (4), 1352−1364.
(120) Deng, L.; Young, R. J.; van der Zwaag, S.; Picken, S. *Polymer* **2010**, *51* (9), 2033−2039.
(121) O'Connor, I.; Hayden, H.; Coleman, J. N.; Gun'ko, Y. K. *Small* **2009**, *5* (4), 466−469.
(122) Chae, H. G.; Choi, Y. H.; Minus, M. L.; Kumar, S. *Compos. Sci. Technol.* **2009**, *69* (3-4), 406−413.

(123) Ko, F.; Gogotsi, Y.; Ali, A.; Naguib, N.; Ye, H.; Yang, G. L.; Li, C.; Willis, P. *Adv. Mater. (Weinheim, Ger.)* **2003**, *15* (14), 1161−1165.
(124) Ye, H.; Lam, H.; Titchenal, N.; Gogotsi, Y.; Ko, F. *Appl. Phys. Lett.* **2004**, *85* (10), 1775−1777.
(125) Maitra, T.; Sharma, S.; Srivastava, A.; Cho, Y.-K.; Madou, M.; Sharma, A. *Carbon* **2012**, *50* (5), 1753−1761.
(126) Sulong, A. B.; Park, J.; Azhari, C. H.; Jusoff, K. *Composites, Part B: Eng.* **2011**, *42* (1), 11−17.
(127) Mezghani, K.; Farooqui, M.; Furquan, S.; Atieh, M. *Mater. Lett.* **2011**, *65* (23-24), 3633−3635.
(128) Rein, D. M.; Cohen, Y.; Lipp, J.; Zussman, E. *Macromol. Mater. Eng.* **2010**, *295* (11), 1003−1008.
(129) Yeh, J.; Lin, S.; Chen, K.; Huang, K. *J. Appl. Polym. Sci.* **2008**, *110* (5), 2538−2548.
(130) Yeh, J.; Wu, T.; Lai, Y.; Zhou, H.; Zhou, Q.; Li, Q.; Wen, S.; Tsai, F.; Huang, C.; Huang, K.; Chen, K. *Polym. Eng. Sci.* **2011**, *51* (4), 687−696.
(131) Khan, M.; Mahfuz, H.; Adnan, A.; Shabib, I.; Leventouri, T. *J. Mater. Eng. Perform.* **2013**, *22* (6), 1593−1600.
(132) Wang, Y.; Cheng, R.; Liang, L.; Wang, Y. *Compos. Sci. Technol.* **2005**, *65* (5), 793−797.
(133) Ruan, S.; Gao, P.; Yu, T. X. *Polymer* **2006**, *47* (5), 1604−1611.
(134) Pötschke, P.; Andres, T.; Villmow, T.; Pegel, S.; Brünig, H.; Kobashi, K.; Fischer, D.; Häussler, L. *Compos. Sci. Technol.* **2010**, *70* (2), 343−349.
(135) Jeong, J. S.; Moon, J. S.; Jeon, S. Y.; Park, J. H.; Alegaonkar, P. S.; Yoo, J. B. *Thin Solid Films* **2007**, *515* (12), 5136−5141.
(136) Bang, H.; Gopiraman, M.; Kim, B.-S.; Kim, S.-H.; Kim, I.-S. *Colloids Surf., A* **2012**, *409* (0), 112−117.
(137) Wong, K. K. H.; Zinke-Allmang, M.; Hutter, J. L.; Hrapovic, S.; Luong, J. H. T.; Wan, W. *Carbon* **2009**, *47* (11), 2571−2578.
(138) Minoo, N.; Lin, T.; Staiger, M. P.; Dai, L.; Wang, X. *Nanotechnology* **2008**, *19* (30), 305702.
(139) Mercader, C.; Denis-Lutard, V.; Jestin, S.; Maugey, M.; Derré, A.; Zakri, C.; Poulin, P. *J. Appl. Polym. Sci.* **2012**, *125* (S1), E191−E196.
(140) Fu, C.; Gu, L. *J. Appl. Polym. Sci.* **2013**, *128* (2), 1044−1053.
(141) Miaudet, P.; Bartholome, C.; Derré, A.; Maugey, M.; Sigaud, G.; Zakri, C.; Poulin, P. *Polymer* **2007**, *48* (14), 4068−4074.
(142) Lachman, N.; Bartholome, C. l.; Miaudet, P.; Maugey, M.; Poulin, P.; Wagner, H. D. *J. Phys. Chem. C* **2009**, *113* (12), 4751−4754.
(143) Blighe, F. M.; Young, K.; Vilatela, J. J.; Windle, A. H.; Kinloch, I. A.; Deng, L.; Young, R. J.; Coleman, J. N. *Adv. Funct. Mater.* **2011**, *21* (2), 364−371.
(144) Young, K.; Blighe, F. M.; Vilatela, J. J.; Windle, A. H.; Kinloch, I. A.; Deng, L.; Young, R. J.; Coleman, J. N. *ACS Nano* **2010**, *4* (11), 6989−6997.
(145) Jee, M.; Choi, J.; Park, S.; Jeong, Y.; Baik, D. *Macromol. Res.* **2012**, *20* (6), 650−657.
(146) Vijaya, K. R.; Yousuf, M.; Jeelani, S.; Pulikkathara, M. X.; Khabashesku, V. N. *Nanotechnology* **2008**, *19* (24), 245703.
(147) Scaffaro, R.; Maio, A.; Tito, A. C. *Compos. Sci. Technol.* **2012**, *72* (15), 1918−1923.
(148) Perrot, C.; Piccione, P. M.; Zakri, C.; Gaillard, P.; Poulin, P. *J. Appl. Polym. Sci.* **2009**, *114* (6), 3515−3523.
(149) Meng, Q.; Wang, Z.; Zhang, X.; Wang, X.; Bai, S. *High Perform. Polym.* **2010**, *22* (7), 848−862.
(150) Gao, J.; Itkis, M. E.; Yu, A.; Bekyarova, E.; Zhao, B.; Haddon, R. C. *J. Am. Chem. Soc.* **2005**, *127* (11), 3847−3854.
(151) Baji, A.; Mai, Y.; Wong, S. *Mater. Sci. Eng., A* **2011**, *528* (21), 6565−6572.
(152) Meng, Q.; Hu, J.; Zhu, Y. *J. Appl. Polym. Sci.* **2007**, *106* (2), 837−848.
(153) Meng, Q.; Hu, J. *Composites, Part A* **2008**, *39* (2), 314−321.
(154) Liu, L. Q.; Tasis, D.; Prato, M.; Wagner, H. D. *Adv. Mater. (Weinheim, Ger.)* **2007**, *19* (9), 1228−1233.
(155) Kim, J. W.; Im, J. S.; Cho, T.; Basova, Y. V.; Edie, D. D.; Lee, Y. S. *J. Ind. Eng. Chem.* **2007**, *13* (5), 757−763.
(156) Andrews, R.; Jacques, D.; Rao, A. M.; Rantell, T.; Derbyshire, F.; Chen, Y.; Chen, J.; Haddon, R. C. *Appl. Phys. Lett.* **1999**, *75* (9), 1329−1331.
(157) Khan, U.; Young, K.; O'Neill, A.; Coleman, J. N. *J. Mater. Chem.* **2012**, *22* (25), 12907−12914.
(158) Sen, K.; Bajaj, P.; Sreekumar, T. V. *J. Polym. Sci., Part B: Polym. Phys.* **2003**, *41* (22), 2949−2958.
(159) Li, J.; Chen, X.; Li, X.; Cao, H.; Yu, H.; Huang, Y. *Polym. Int.* **2006**, *55* (4), 456−465.
(160) Hu, Z.; Li, J.; Tang, P.; Li, D.; Song, Y.; Li, Y.; Zhao, L.; Li, C.; Huang, Y. *J. Mater. Chem.* **2012**, *22* (37), 19863−19871.
(161) Zhou, C.; Wang, S.; Zhang, Y.; Zhuang, Q.; Han, Z. *Polymer* **2008**, *49* (10), 2520−2530.
(162) Spinks, G. M.; Mottaghitalab, V.; Bahrami-Samani, M.; Whitten, P. G.; Wallace, G. G. *Adv. Mater. (Weinheim, Ger.)* **2006**, *18* (5), 637−640.
(163) Kumar, S.; Doshi, H.; Srinivasarao, M.; Park, J. O.; Schiraldi, D. A. *Polymer* **2002**, *43* (5), 1701−1703.
(164) McIntosh, D.; Khabashesku, V. N.; Barrera, E. V. *J. Phys. Chem. C* **2007**, *111* (4), 1592−1600.
(165) McIntosh, D.; Khabashesku, V. N.; Barrera, E. V. *Chem. Mater.* **2006**, *18* (19), 4561−4569.
(166) Soitong, T.; Pumchusak, J. *J. Appl. Polym. Sci.* **2011**, *119* (2), 962−967.
(167) Kearns, J. C.; Shambaugh, R. L. *J. Appl. Polym. Sci.* **2002**, *86* (8), 2079−2084.
(168) Moore, E. M.; Ortiz, D. L.; Marla, V. T.; Shambaugh, R. L.; Grady, B. P. *J. Appl. Polym. Sci.* **2004**, *93* (6), 2926−2933.
(169) Liu, Z. H.; Pan, C. T.; Lin, L. W.; Lai, H. W. *Sens. Actuators A: Phys.* **2013**, *193* (0), 13−24.
(170) Guo, Z.; Nilsson, E.; Rigdahl, M.; Hagström, B. *J. Appl. Polym. Sci.* **2013**, *130* (4), 2603−2609.
(171) Teng, N. Y.; Dallmeyer, I.; Kadla, J. F. *J. Wood Chem. Technol.* **2013**, *33* (4), 299−316.
(172) Muñoz, E.; Suh, D. S.; Collins, S.; Selvidge, M.; Dalton, A. B.; Kim, B. G.; Razal, J. M.; Ussery, G.; Rinzler, A. G.; Martínez, M. T.; Baughman, R. H. *Adv. Mater. (Weinheim, Ger.)* **2005**, *17* (8), 1064−1067.
(173) Siochi, E. J.; Working, D. C.; Park, C.; Lillehei, P. T.; Rouse, J. H.; Topping, C. C.; Bhattacharyya, A. R.; Kumar, S. *Composites, Part B* **2004**, *35* (5), 439−446.
(174) Chatterjee, S.; Nüesch, F. A.; Chu, B. T. T. *Chem. Phys. Lett.* **2013**, *557* (0), 92−96.
(175) Saligheh, O.; Forouharshad, M.; Arasteh, R.; Eslami-Farsani, R.; Khajavi, R.; Yadollah Roudbari, B. *J. Polym. Res.* **2013**, *20* (2), 1−6.
(176) Guan, W.; Tan, Z.; Liu, X.; Chawda, S.; Koo, J.; Samuilov, V.; Dudley, M. *Nanotechnology* **2006**, *17* (23), 5829.
(177) Dror, Y.; Salalha, W.; Khalfin, R. L.; Cohen, Y.; Yarin, A. L.; Zussman, E. *Langmuir* **2003**, *19* (17), 7012−7020.
(178) Khan, W. S.; Asmatulu, R.; Eltabey, M. M. *J. Nanomaterials* **2013**, *2013*, 9−9.
(179) Im, J. S.; Kim, J. G.; Lee, S.-H.; Lee, Y.-S. *Colloids Surf., A* **2010**, *364* (1-3), 151−157.
(180) Lin, Y.; Wu, T. *J. Appl. Polym. Sci.* **2012**, *126* (S2), E123−E129.
(181) Hooshmand, S.; Soroudi, A.; Skrifvars, M. *Synth. Met.* **2011**, *161* (15-16), 1731−1737.
(182) Putz, K. W.; Mitchell, C. A.; Krishnamoorti, R.; Green, P. F. *J. Polym. Sci., Part B: Polym. Phys.* **2004**, *42* (12), 2286−2293.
(183) Xu, X.; Thwe, M. M.; Shearwood, C.; Liao, K. *Appl. Phys. Lett.* **2002**, *81* (15), 2833−2835.